Dissertation Defense

Enabling High-Order Methods for Extreme-Scale Simulations

February 9, 2018

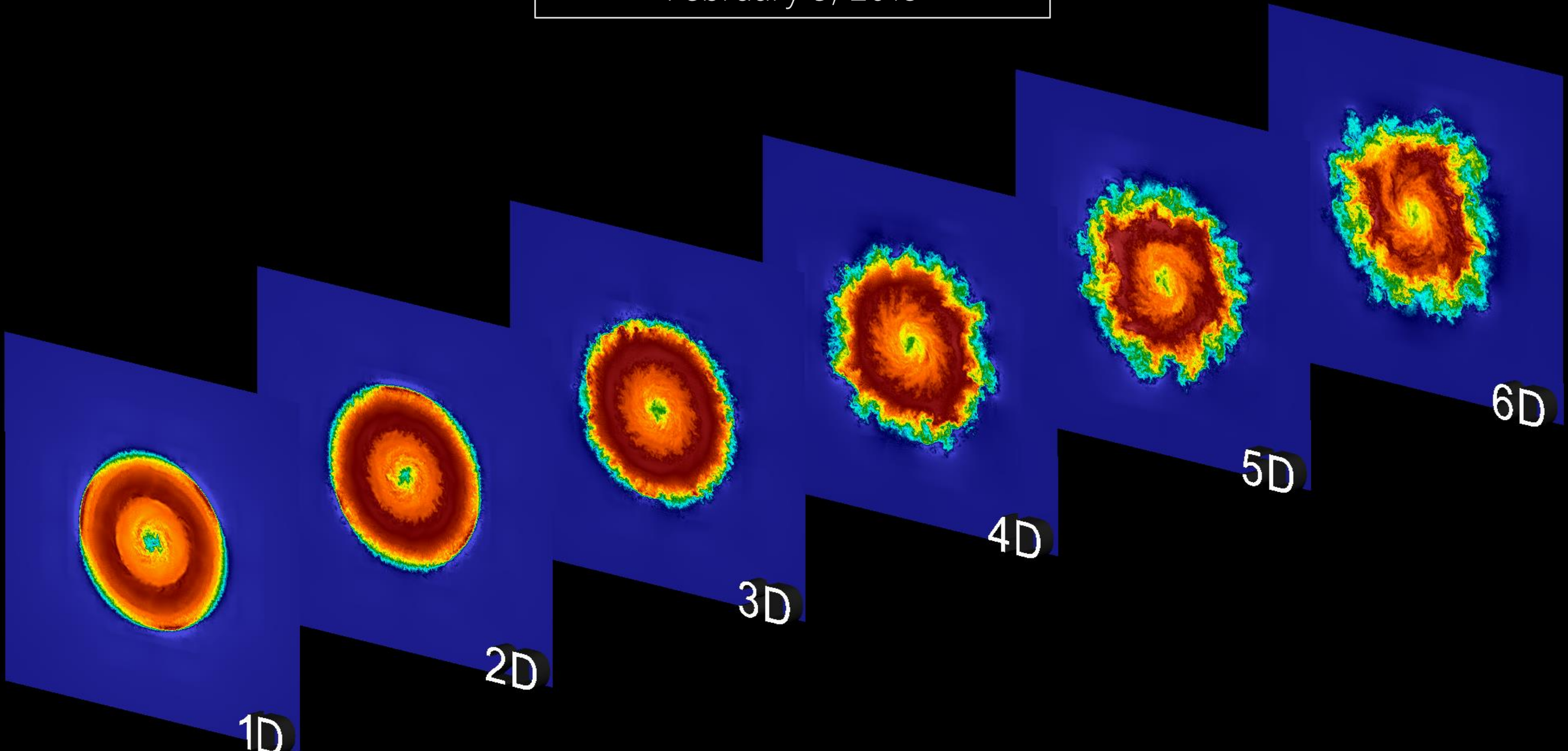

COLLEGE OF ENGINEERING & APPLIED SCIENCE
UNIVERSITY of WYOMING

Andrew C. Kirby

Department of Mechanical Engineering
University of Wyoming

COLLEGE OF ENGINEERING & APPLIED SCIENCE
UNIVERSITY of WYOMING

Committee

Dr. Dimitri Mavriplis

Dr. Victor Ginting

Dr. Jonathan Naughton

Dr. Jay Sitaraman Parallel Geometric Algorithms, LLC

Dr. Marc Spiegelman Columbia University

To Elizabeth J. Gilbert

(1951-2016)

Motivation

Can high-order CFD methods be used for extreme-scale simulations?

- What do we mean by high-order methods? Why do we need them?
- What do we mean by extreme-scale simulations?

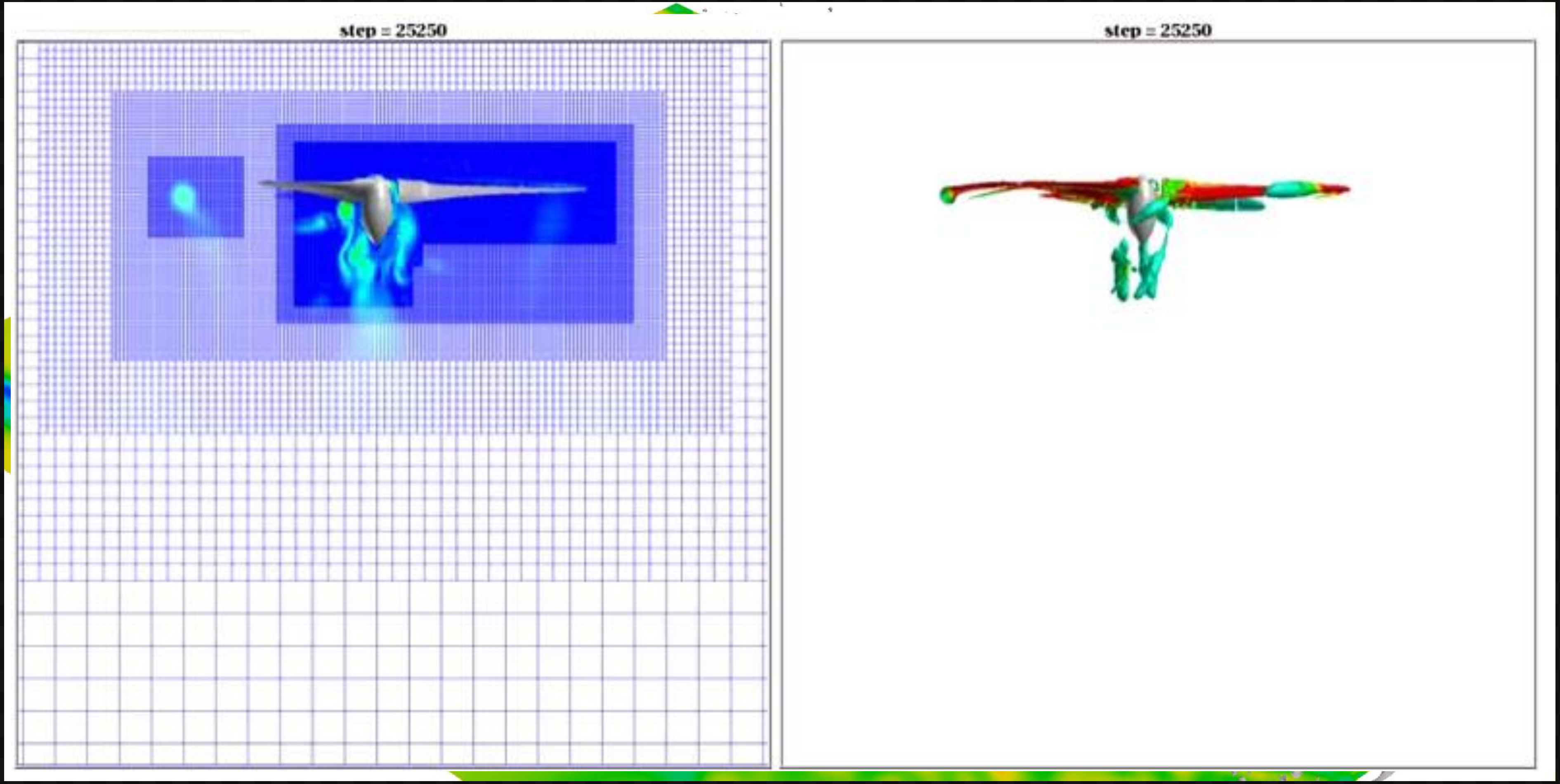

CREATE-AV HELIOS

COLLEGE OF ENGINEERING & APPLIED SCIENCE
UNIVERSITY OF WYOMING

Motivation

Can high-order CFD methods be used for extreme-scale simulations?

- What do we mean by high-order methods? Why do we need them?
- What do we mean by extreme-scale simulations?

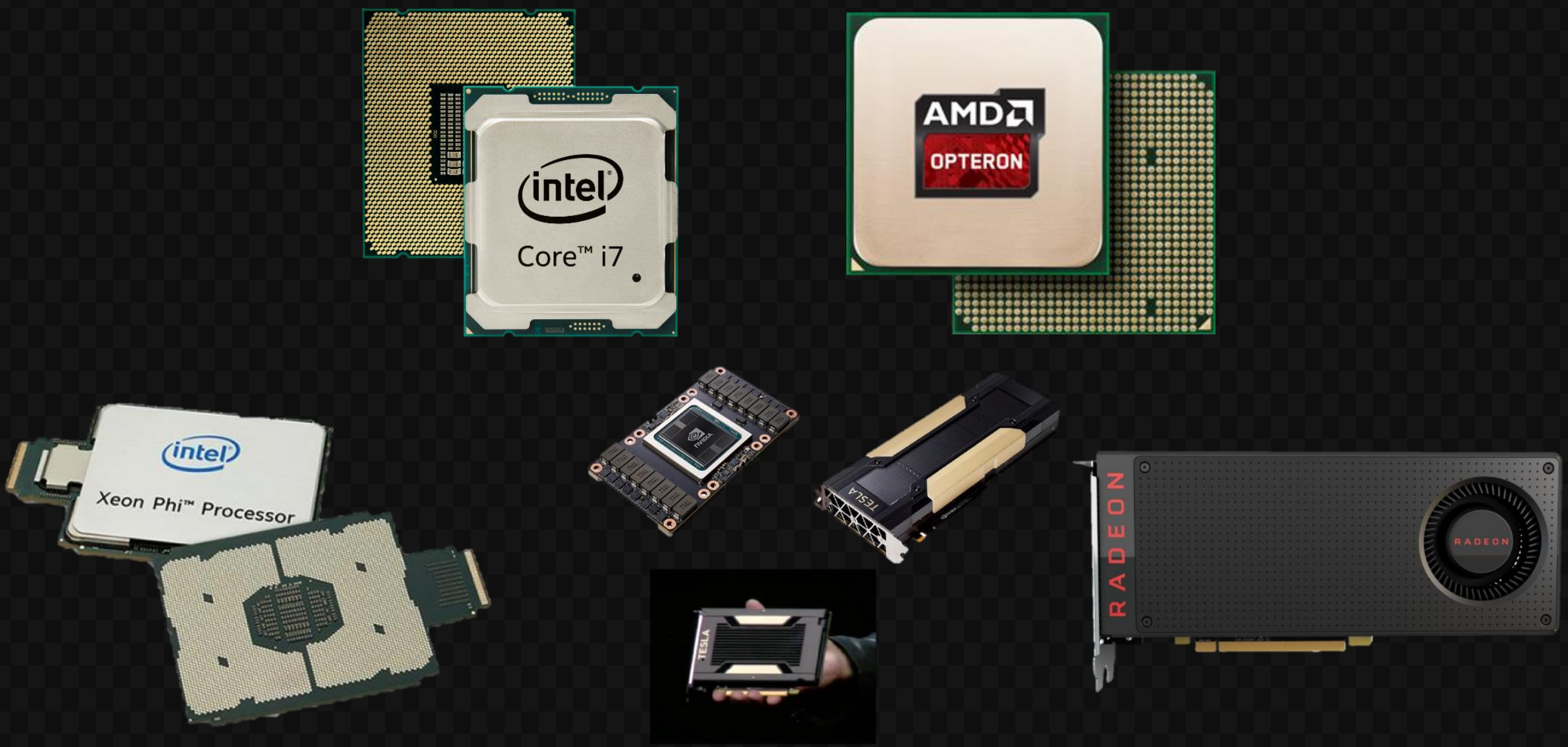

NVIDIA V100
7.8 TFLOPS Double Precision

Challenges

Traditional High-Order Method Challenges

- Computationally Costly
  - general FEM construction
- Stability Issues
  - ad-hoc correction
- Multiscale Challenges
  - unstructured methods (generally 2^{nd} order)
  - FD, HO FV stencils for AMR

Motivation

Governing Equations

Discretization

Goals

Results

Conclusions

Future Work

Governing Equations

Compressible Navier-Stokes Equations

$$\frac{\partial \mathbf{Q}\left(\boldsymbol{x},t\right)}{\partial t} + \vec{\nabla} \cdot \mathbf{F}\left(\mathbf{Q}\left(\boldsymbol{x},t\right)\right) = 0$$

$$\mathbf{Q} = \begin{Bmatrix} \rho \\ \rho u \\ \rho v \\ \rho w \\ \rho E \end{Bmatrix}, \mathbf{F} = \begin{array}{c} \begin{array}{ccc} \underline{\mathbf{F}^1} & \underline{\mathbf{F}^2} & \underline{\mathbf{F}^3} \end{array} \\ \begin{Bmatrix} \rho u & \rho v & \rho w \\ \rho u^2 + p - \tau_{11} & \rho u v - \tau_{12} & \rho u w - \tau_{13} \\ \rho u v - \tau_{21} & \rho v^2 + p - \tau_{22} & \rho v w - \tau_{23} \\ \rho u w - \tau_{31} & \rho v w - \tau_{32} & \rho w^2 + p - \tau_{33} \\ \rho u H + q_1 - \tau_{1j} u_j & \rho v H + q_2 - \tau_{2j} u_j & \rho w H + q_3 - \tau_{3j} u_j \end{Bmatrix} \end{array}$$

Governing Equations

Continuous to Discrete

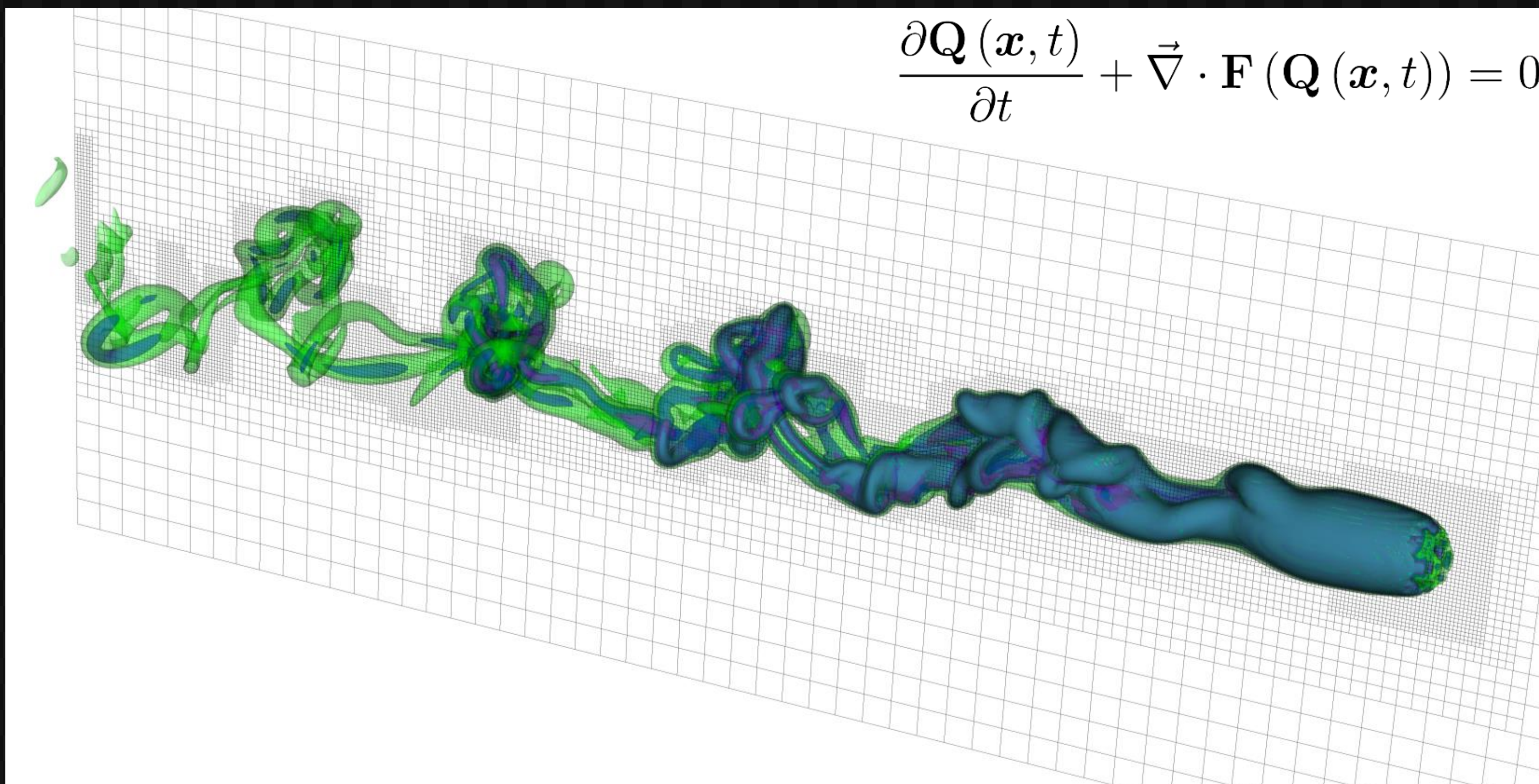

$$\frac{\partial \mathbf{Q}\left(\boldsymbol{x},t\right)}{\partial t} + \vec{\nabla} \cdot \mathbf{F}\left(\mathbf{Q}\left(\boldsymbol{x},t\right)\right) = 0$$

Motivation

Governing Equations

Discretization

Goals

Results

Conclusions

Future Work

Discretization

$$\frac{\partial \mathbf{Q}\left(\boldsymbol{x},t\right)}{\partial t} + \vec{\nabla} \cdot \mathbf{F}\left(\mathbf{Q}\left(\boldsymbol{x},t\right)\right) = 0$$

Finite Element Method

$$\boxed{}\left(\boxed{\frac{\partial \mathbf{Q}}{\partial t}} + \boxed{\vec{\nabla} \cdot \mathbf{F}}\right)\boxed{}\,\boxed{} = 0$$

$$\boxed{- \boxed{\int_{\Omega_k} \left(\mathbf{F} \cdot \vec{\nabla}\right) \psi(\boldsymbol{x}) \mathrm{d}\boldsymbol{x}} + \boxed{\int_{\Gamma_k} \left(\mathbf{F}^* \cdot \vec{\mathrm{n}}\right) \psi(\boldsymbol{x}|_{\Gamma_k}) \mathrm{d}\Gamma_k}}$$

I II III

1.) Multiply by test function
2.) Integrate over mesh element
3.) Integrate by parts once

I. Temporal Derivative Integral
II. Weak Form Volume Integral
III. Surface Integral

Discretization

$$\frac{\partial \mathbf{Q}\left(\boldsymbol{x},t\right)}{\partial t} + \vec{\nabla} \cdot \mathbf{F}\left(\mathbf{Q}\left(\boldsymbol{x},t\right)\right) = 0$$

Finite Element Method

$$\boxed{\int_{\Omega_k}} \left(\boxed{\frac{\partial \mathbf{Q}}{\partial t}} + \boxed{\vec{\nabla} \cdot \mathbf{F}} \right) \boxed{\psi(\boldsymbol{x})} \boxed{\mathrm{d}\boldsymbol{x}} = 0$$

$$\mathbf{R}^{\mathrm{Weak}} = \underbrace{\int_{\Omega_k} \frac{\partial \mathbf{Q}}{\partial t} \psi(\boldsymbol{x}) \mathrm{d}\boldsymbol{x}}_{\mathrm{I}} \underbrace{- \int_{\Omega_k} \left(\mathbf{F} \cdot \vec{\nabla}\right) \psi(\boldsymbol{x}) \mathrm{d}\boldsymbol{x}}_{\mathrm{II}} + \underbrace{\int_{\Gamma_k} \left(\mathbf{F}^* \cdot \vec{\mathrm{n}}\right) \psi(\boldsymbol{x}|_{\Gamma_k}) \mathrm{d}\Gamma_k}_{\mathrm{III}} = 0$$

1.) Multiply by test function
2.) Integrate over mesh element
3.) Integrate by parts once

I. Temporal Derivative Integral

II. Weak Form Volume Integral

III. Surface Integral

Test and Basis Functions

$$\psi(x)$$

Modal

$$\phi_s(x) \rightarrow \phi_s(x) = x^{s-1}$$

Nodal

$$\ell_s(x) \rightarrow \ell_s(x) = \prod_{i=1, i \neq s}^{N} \frac{(x - \xi_i)}{(\xi_s - \xi_i)}$$

Lagrange Interpolating Polynomial
One-Dimensional

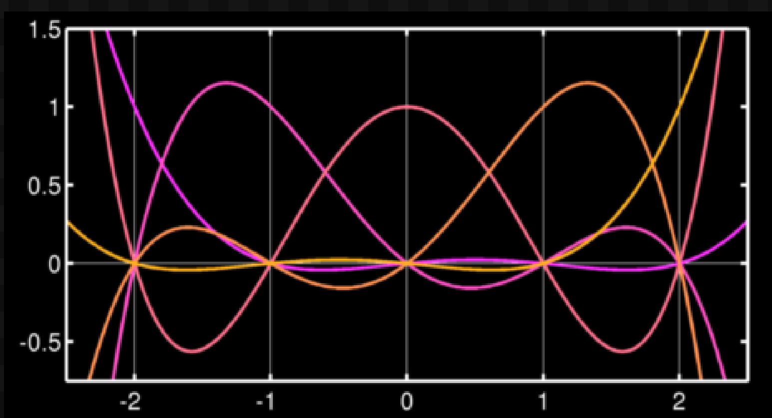

$$\ell_s(\xi_i) = \delta_{si} = \begin{cases} 0, & s \neq i \\ 1, & s = i \end{cases}$$

$$\psi(x) = \ell_i(\xi^1)\ell_j(\xi^2)\ell_k(\xi^3)$$

Solution Expansion

$$\psi(\boldsymbol{x})$$

Solution Expansion

$$\mathbf{Q}(\boldsymbol{\xi}, t) =$$
$$=$$
$$=$$

$$\ell_s(\xi_i) = \delta_{si} = \begin{cases} 0, & s \neq i \\ 1, & s = i \end{cases}$$

$$\ell_i(\xi_\lambda)\omega_\lambda = \delta_{i\lambda}\omega_\lambda = \omega_i$$

$$u\left(\xi_i\right) = \sum_{s=1}^{N} u_s \ell_s\left(\xi_i\right) = \sum_{s=1}^{N} u_s \delta_{si} = u_i$$

Gauss Legendre

Gauss Lobatto Legendre

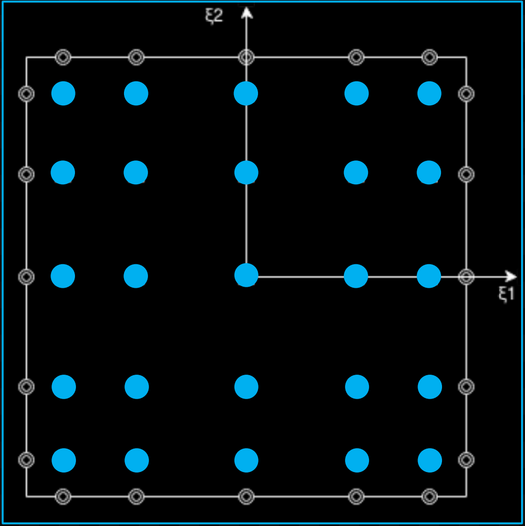

Solution Expansion

$$\psi(\boldsymbol{x})$$

Solution Expansion

$$\begin{aligned}\mathbf{Q}(\boldsymbol{\xi},t) &= \sum_{s=1}^{N^3} \tilde{\mathbf{Q}}_s(t)\psi_s(\boldsymbol{\xi}) \\ &= \sum_{l=1}^{N} \ell_l(\xi^3)\left[\sum_{n=1}^{N} \ell_n(\xi^2)\left[\sum_{m=1}^{N} \mathbf{Q}_{mnl}(t)\ell_m(\xi^1)\right]\right] \\ &= \sum_{m,n,l=1}^{N} \mathbf{Q}_{mnl}(t)\ell_m(\xi^1)\ell_n(\xi^2)\ell_l(\xi^3)\end{aligned}$$

$$\ell_s(\xi_i) = \delta_{si} = \begin{cases} 0, & s \neq i \\ 1, & s = i \end{cases}$$

$$\ell_i(\xi_\lambda)\omega_\lambda = \delta_{i\lambda}\omega_\lambda = \omega_i$$

$$u(\xi_i) = \sum_{s=1}^{N} u_s \ell_s(\xi_i) = \sum_{s=1}^{N} u_s \delta_{si} = u_i$$

Gauss Legendre

Gauss Lobatto Legendre

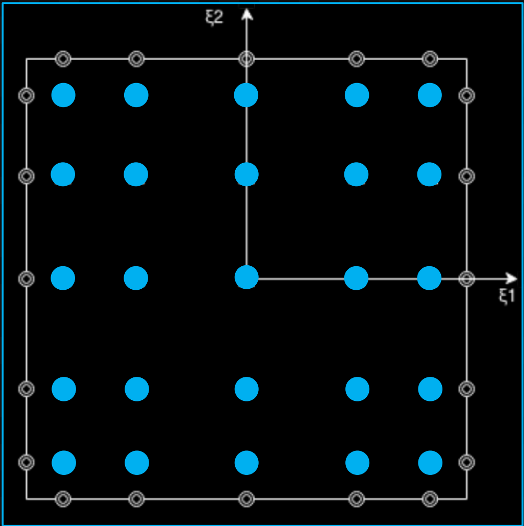

Numerical Integration

$$\int_{\Omega_k} \frac{\partial Q}{\partial t} \psi(x) \, \mathrm{d}x$$

$$\int_{-1}^{1} f(x)dx = \sum_{i=1}^{n} \omega_i f(\xi_i)$$

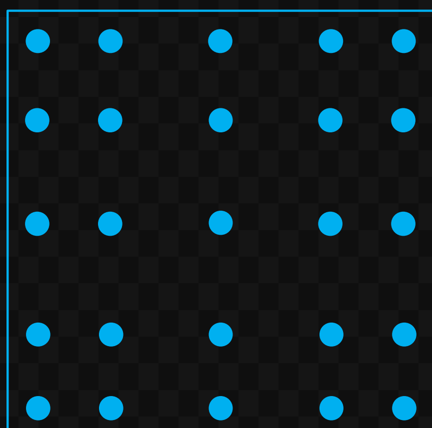

Gauss Legendre

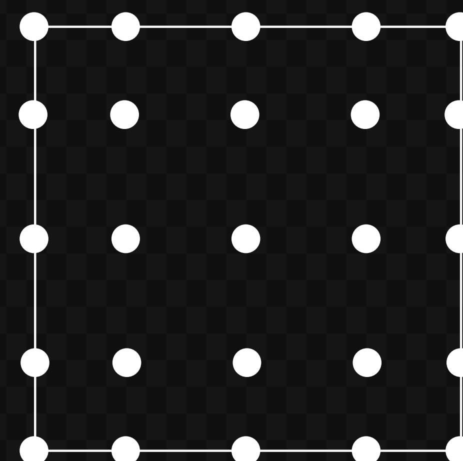

Gauss Lobatto Legendre

<u>Collocation</u>

Solution Points = Integration Points

$$\boxed{\mathbf{R}^{\text{Weak}} = \underbrace{\boxed{\int_{\Omega_k} \frac{\partial \mathbf{Q}}{\partial t} \psi(\boldsymbol{x}) \mathrm{d}\boldsymbol{x}}}_{\mathbf{I}} \boxed{- \underbrace{\boxed{\int_{\Omega_k} \left(\mathbf{F} \cdot \vec{\nabla}\right) \boldsymbol{\psi}(\boldsymbol{x}) \mathrm{d}\boldsymbol{x}}}_{\mathbf{II}} + \underbrace{\boxed{\int_{\Gamma_k} \left(\mathbf{F}^* \cdot \vec{\mathrm{n}}\right) \boldsymbol{\psi}(\boldsymbol{x}|_{\Gamma_k}) \mathrm{d}\Gamma_k}}_{\mathbf{III}}} = 0}$$

Term I

$$\int_{\Omega_k} \frac{\partial \mathbf{Q}}{\partial t}\psi(\boldsymbol{x})\mathrm{d}\boldsymbol{x}$$

$$\int_E \frac{\partial \mathbf{Q}}{\partial t}\psi J(\boldsymbol{\xi})\mathrm{d}\boldsymbol{\xi} = \frac{\partial}{\partial t}\int_E \boxed{\mathbf{Q}}\boxed{\psi} J(\boldsymbol{\xi})\mathrm{d}\boldsymbol{\xi}$$

$$\mathbf{Q}(\boldsymbol{\xi},t) = \sum_{m,n,l=1}^{N} \mathbf{Q}_{mnl}(t)\ell_m(\xi^1)\ell_n(\xi^2)\ell_l(\xi^3)$$

$$\boldsymbol{\psi}(\boldsymbol{x}) = \ell_i(\xi^1)\ell_j(\xi^2)\ell_k(\xi^3)$$

$$\frac{\partial}{\partial t}\int_E \mathbf{Q}\psi J(\boldsymbol{\xi})\mathrm{d}\boldsymbol{\xi} = \frac{\partial}{\partial t}\boxed{\int_E}\underbrace{\left(\sum_{m,n,l=1}^{N} \mathbf{Q}_{mnl}(t)\ell_m(\xi^1)\ell_n(\xi^2)\ell_l(\xi^3)\right)}_{\boxed{\mathbf{Q}}}\underbrace{\ell_i(\xi^1)\ell_j(\xi^2)\ell_k(\xi^3)}_{\boxed{\psi}} J(\boldsymbol{\xi})\boxed{\mathrm{d}\boldsymbol{\xi}}$$

$$\int_{-1}^{1} f(x)dx = \sum_{i=1}^{n}\omega_i f(\xi_i)$$

$$\approx \frac{\partial}{\partial t}\boxed{\sum_{\lambda,\mu,\nu=1}^{N}}\left(\sum_{m,n,l=1}^{N}\mathbf{Q}_{mnl}(t)\boxed{\ell_m(\xi^1_\lambda)\ell_n(\xi^2_\mu)\ell_l(\xi^3_\nu)}\right)\boxed{\ell_i(\xi^1_\lambda)\ell_j(\xi^2_\mu)\ell_k(\xi^3_\nu)}J(\xi^1_\lambda,\xi^2_\mu,\xi^3_\nu)\boxed{\omega_\lambda\omega_\mu\omega_\nu}$$

$$\ell_s(\xi_i) = \delta_{si} = \begin{cases} 0, & s \neq i \\ 1, & s = i \end{cases}$$

Term I

$$\boxed{\int_{\Omega_k} \frac{\partial \mathbf{Q}}{\partial t}\psi(\boldsymbol{x})\mathrm{d}\boldsymbol{x}}$$

$$\int_E \frac{\partial \mathbf{Q}}{\partial t}\psi J(\boldsymbol{\xi})\mathrm{d}\boldsymbol{\xi} = \frac{\partial}{\partial t}\int_E \mathbf{Q}\psi J(\boldsymbol{\xi})\mathrm{d}\boldsymbol{\xi}$$

$$\frac{\partial}{\partial t}\sum_{\lambda,\mu,\nu=1}^{N}\left(\sum_{m,n,l=1}^{N}\mathbf{Q}_{mnl}\underbrace{\ell_m(\xi^1_\lambda)}_{=\delta_{m\lambda}}\underbrace{\ell_n(\xi^2_\mu)}_{=\delta_{n\mu}}\underbrace{\ell_l(\xi^3_\nu)}_{=\delta_{l\nu}}\right)\underbrace{\ell_i(\xi^1_\lambda)}_{=\delta_{i\lambda}}\underbrace{\ell_j(\xi^2_\mu)}_{=\delta_{j\mu}}\underbrace{\ell_k(\xi^3_\nu)}_{=\delta_{k\nu}}J(\xi^1_\lambda,\xi^2_\mu,\xi^3_\nu)\omega_\lambda\omega_\mu\omega_\nu$$

$$\ell_i(\xi_\lambda)\omega_\lambda = \delta_{i\lambda}\omega_\lambda = \omega_i$$

$$= \frac{\partial}{\partial t}\sum_{\lambda,\mu,\nu=1}^{N}\mathbf{Q}_{\lambda\mu\nu}\underbrace{\ell_i(\xi^1_\lambda)}_{=\delta_{i\lambda}}\underbrace{\ell_j(\xi^2_\mu)}_{=\delta_{j\mu}}\underbrace{\ell_k(\xi^3_\nu)}_{=\delta_{k\nu}}J(\xi^1_\lambda,\xi^2_\mu,\xi^3_\nu)\omega_\lambda\omega_\mu\omega_\nu$$

by: $\underbrace{\delta_{m\lambda}}_{m\to\lambda}, \underbrace{\delta_{n\mu}}_{n\to\mu}, \underbrace{\delta_{l\nu}}_{l\to\nu}$

$$= J(\xi^1_i,\xi^2_j,\xi^3_k)\omega_i\omega_j\omega_k\frac{\partial \mathbf{Q}_{ijk}}{\partial t}$$

by: $\underbrace{\delta_{\lambda i}}_{\lambda\to i}, \underbrace{\delta_{\mu j}}_{\mu\to j}, \underbrace{\delta_{\nu k}}_{\nu\to k}$

Temporal Derivative Integral:

$$\int_{\Omega_k} \frac{\partial \mathbf{Q}}{\partial t}\psi(\boldsymbol{x})\mathrm{d}\boldsymbol{x} = \mathrm{M}\frac{\partial \mathbf{Q}_{ijk}}{\partial t}$$

$$\mathrm{M} = M_{ijk} = J\omega_i\omega_j\omega_k$$

Term II

$$\int_{\Omega_k}\left(\mathbf{F}\cdot\vec{\nabla}\right)\psi(\boldsymbol{x})\mathrm{d}\boldsymbol{x}$$

$$\int_{\Omega_k}\left(\mathbf{F}(\mathbf{Q})\cdot\vec{\nabla}\right)\psi(\boldsymbol{x})\mathrm{d}\boldsymbol{x} = \sum_{d=1}^{3}\int_E \boxed{\mathcal{F}^d(\mathbf{Q}(\boldsymbol{\xi}))}\frac{\partial\psi(\boldsymbol{\xi})}{\partial\xi^d}\mathrm{d}\boldsymbol{\xi}$$

$$\mathcal{F}^d(\mathbf{Q}(\boldsymbol{\xi})) = \sum_{m,n,l=1}^{N}\tilde{\mathcal{F}}^d_{mnl}\ell_m(\xi^1)\ell_n(\xi^2)\ell_l(\xi^3)$$

Weak Formulation Volume Integral:

$$\int_{\Omega_k}\left(\mathbf{F}(\mathbf{Q})\cdot\vec{\nabla}\right)\psi(\boldsymbol{x})\mathrm{d}\boldsymbol{x} = \omega_j\omega_k\sum_{\lambda=1}^{N}\overline{D}_{i\lambda}\tilde{\mathcal{F}}^1_{\lambda jk}\omega_\lambda + \omega_i\omega_k\sum_{\mu=1}^{N}\overline{D}_{j\mu}\tilde{\mathcal{F}}^2_{i\mu k}\omega_\mu + \omega_i\omega_j\sum_{\nu=1}^{N}\overline{D}_{k\nu}\tilde{\mathcal{F}}^3_{ij\nu}\omega_\nu$$

$$\overline{D}_{ij} = \frac{\mathrm{d}\ell_i(\xi_j)}{\mathrm{d}\xi}, \quad i,j = 0,\ldots,N$$

Term III

$$\int_{\Gamma_k} \left(\mathbf{F}^* \cdot \vec{\mathrm{n}}\right) \boldsymbol{\psi}(\boldsymbol{x}|_{\Gamma_k}) \mathrm{d}\Gamma_k$$

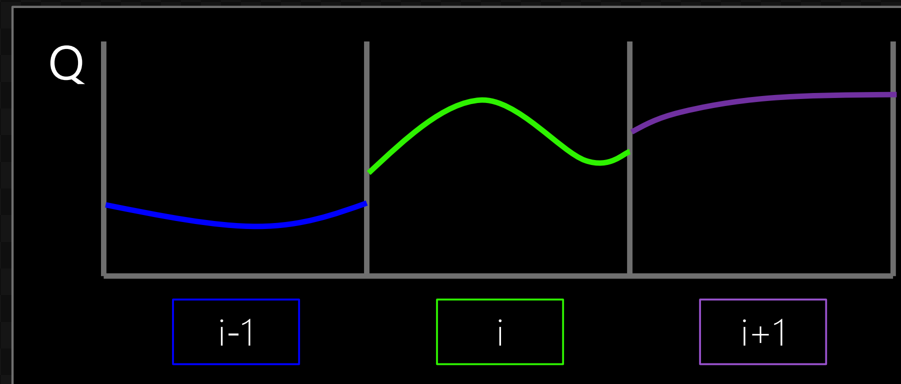

Inviscid Flux
Lax Friedrichs

Viscous Flux
Symmetric Interior Penalty

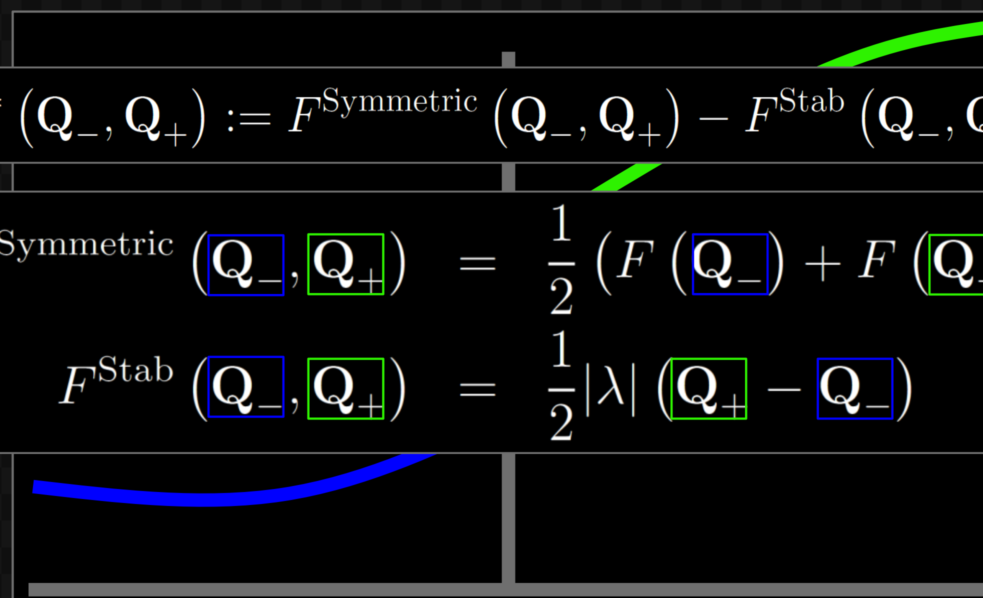

$$F^* \left(\mathbf{Q}_-, \mathbf{Q}_+\right) := F^{\text{Symmetric}} \left(\mathbf{Q}_-, \mathbf{Q}_+\right) - F^{\text{Stab}} \left(\mathbf{Q}_-, \mathbf{Q}_+\right)$$

$$F^{\text{Symmetric}} \left(\boxed{\mathbf{Q}_-}, \boxed{\mathbf{Q}_+}\right) = \frac{1}{2} \left(F\left(\boxed{\mathbf{Q}_-}\right) + F\left(\boxed{\mathbf{Q}_+}\right)\right)$$

$$F^{\text{Stab}} \left(\boxed{\mathbf{Q}_-}, \boxed{\mathbf{Q}_+}\right) = \frac{1}{2} |\lambda| \left(\boxed{\mathbf{Q}_+} - \boxed{\mathbf{Q}_-}\right)$$

Term III

$$\int_{\Gamma_k} (\mathbf{F}^* \cdot \vec{\mathrm{n}})\, \boldsymbol{\psi}(\boldsymbol{x}|_{\Gamma_k}) \mathrm{d}\Gamma_k$$

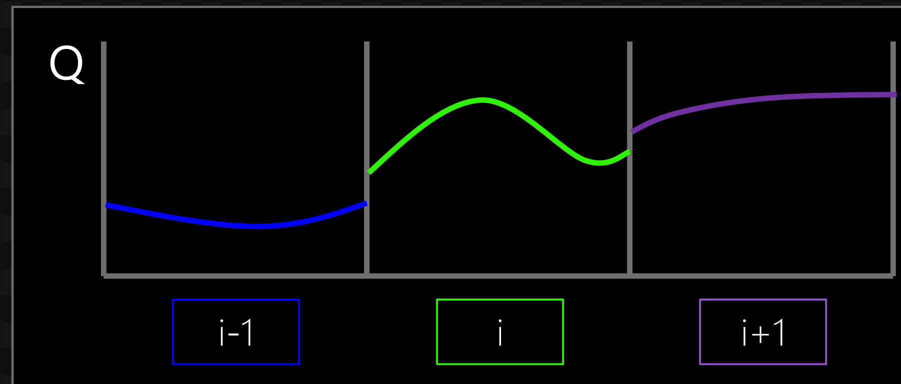

Surface Integral:

$$\boxed{\int_{\Gamma} (\mathbf{F}^* \cdot \vec{\mathrm{n}})\, \boldsymbol{\psi} \mathrm{d}\Gamma} = \left(\tilde{\mathcal{F}}^*_{(+1)jk} \ell_i(+1) - \tilde{\mathcal{F}}^*_{(-1)jk} \ell_i(-1)\right) \omega_j \omega_k$$
$$+ \left(\tilde{\mathcal{F}}^*_{i(+1)k} \ell_j(+1) - \tilde{\mathcal{F}}^*_{i(-1)k} \ell_j(-1)\right) \omega_i \omega_k$$
$$+ \left(\tilde{\mathcal{F}}^*_{ij(+1)} \ell_k(+1) - \tilde{\mathcal{F}}^*_{ij(-1)} \ell_k(-1)\right) \omega_i \omega_j$$

Semi-Discrete Formulation

$$\mathbb{M}\frac{\partial \mathbf{Q}_{ijk}(t)}{\partial t} + \mathbf{R}_{ijk}\left(\mathbf{Q}\right) = 0$$

$$\frac{dy}{dt} = f(t, y), \quad y(t_0) = y_0$$

Explicit Runge-Kutta Methods

- 2-Stage, 2nd-Order SSP-TVD RK2
- 3-Stage, 3rd-Order SSP-TVD RK3
- 4-Stage, 4th-Order RK 3/8-rule

Verification

Ringleb Flow

- Exact solution of 2D Inviscid equations
- Asymptotic error reduction

$$Ch^{p+1}$$

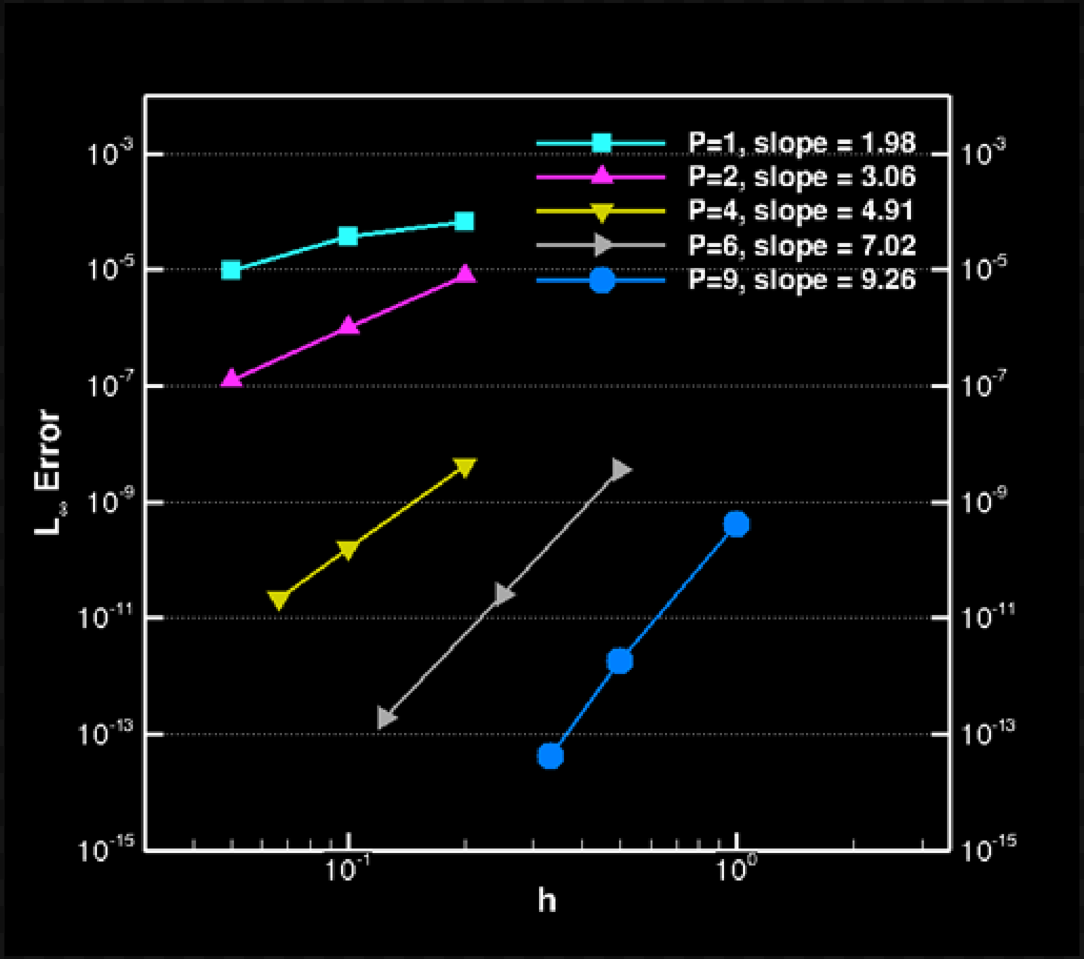

Verification

Taylor-Green Vortex

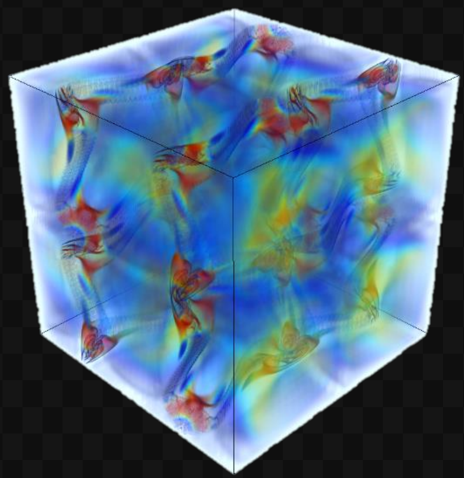

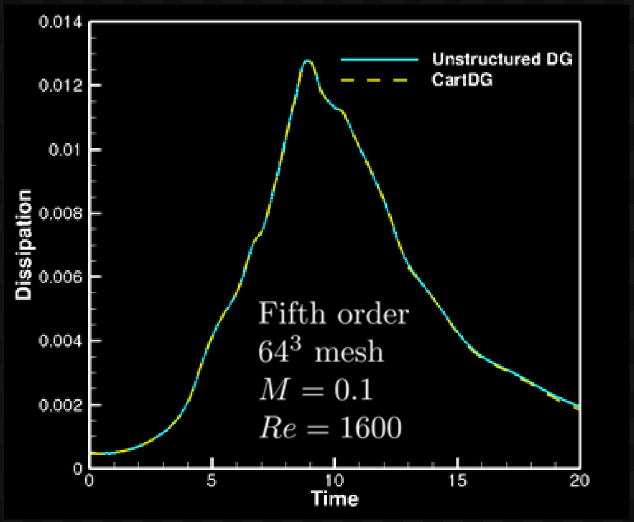

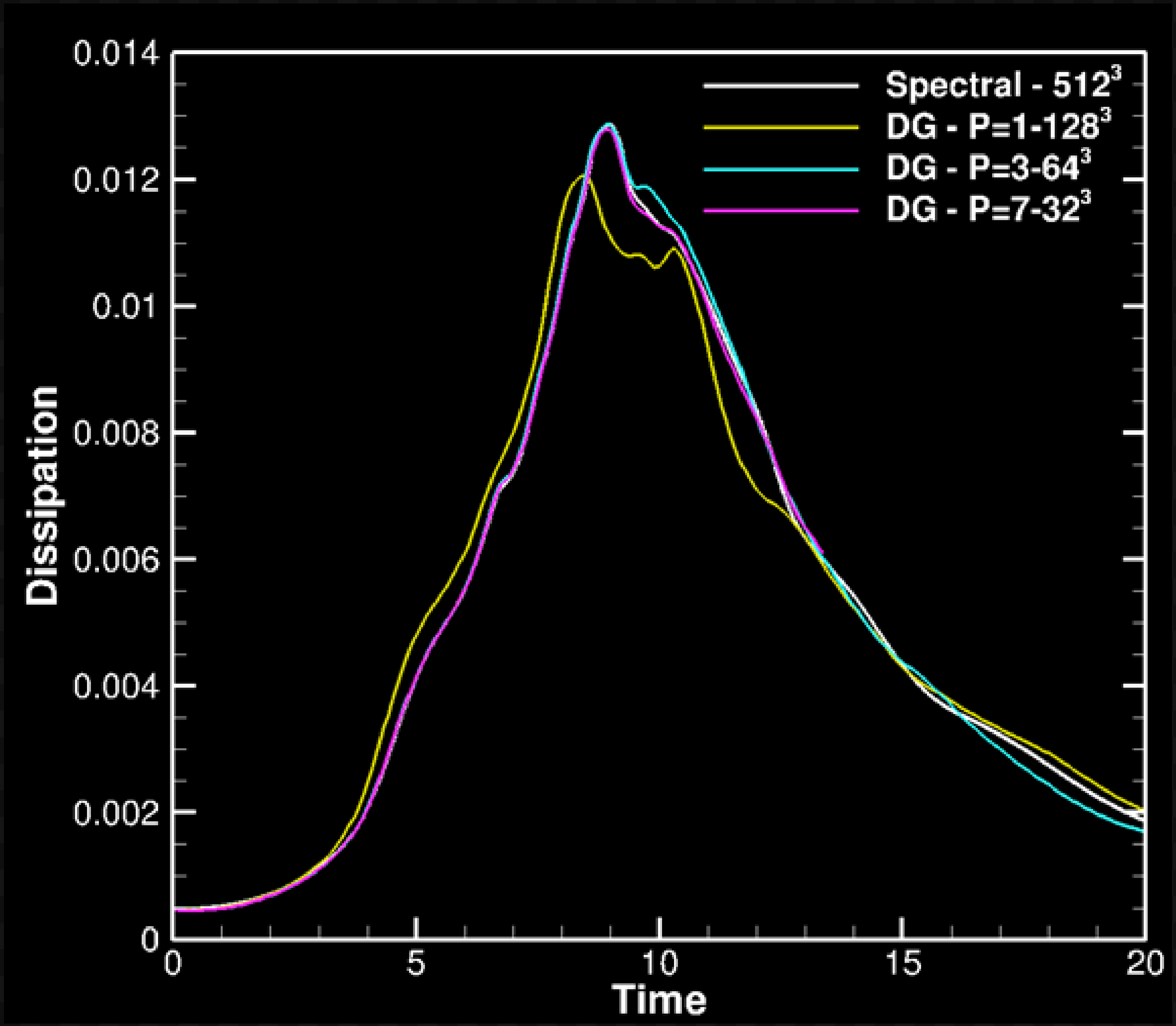

Motivation
Governing Equations
Discretization
Goals
Results
Conclusions
Future Work

Goals

Develop High-Order CFD Method

- Computationally Efficient
- Parallel Scalable
- Robust
- Multiscale
- Real Applications

Goals

Develop High-Order CFD Method

- Computationally Efficient
- Parallel Scalable
- Robust
- Multiscale
- Real Applications

Computational Efficiency

General Basis vs Tensor Basis

Peak Performance

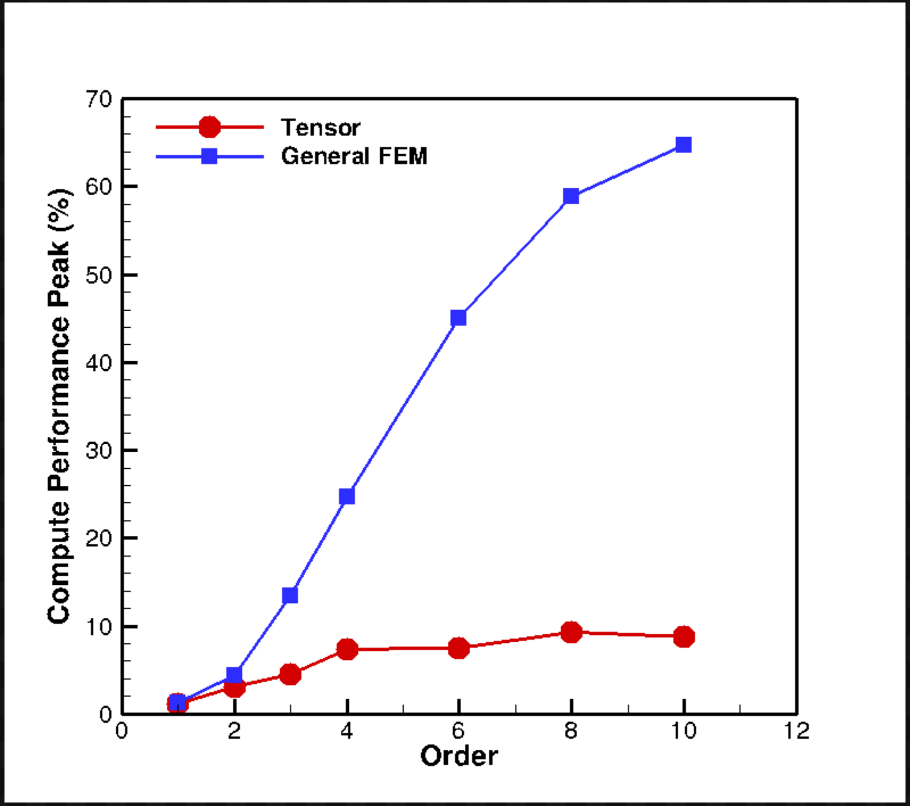

Time Per DOF

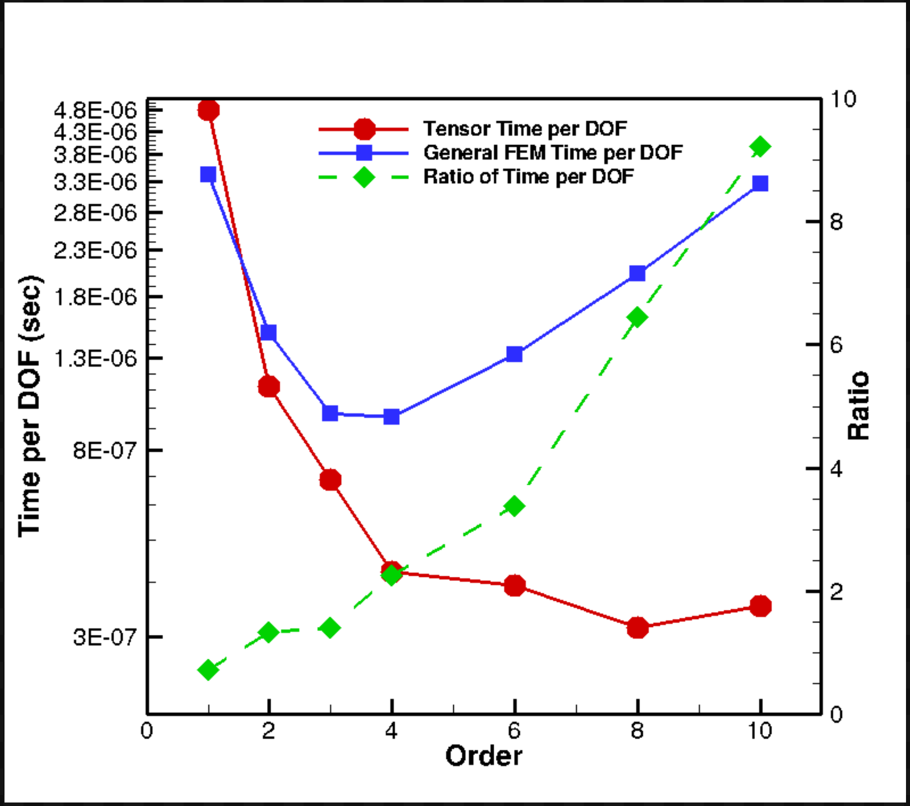

Computational Efficiency

Viscous vs Inviscid

Peak Performance

Time Per DOF

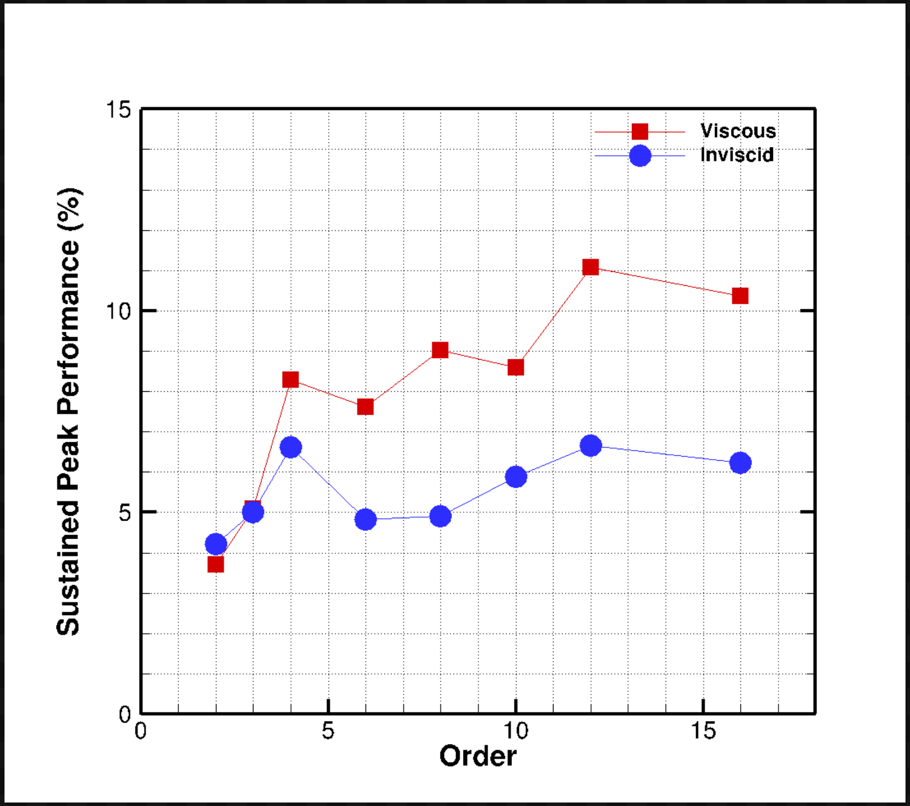

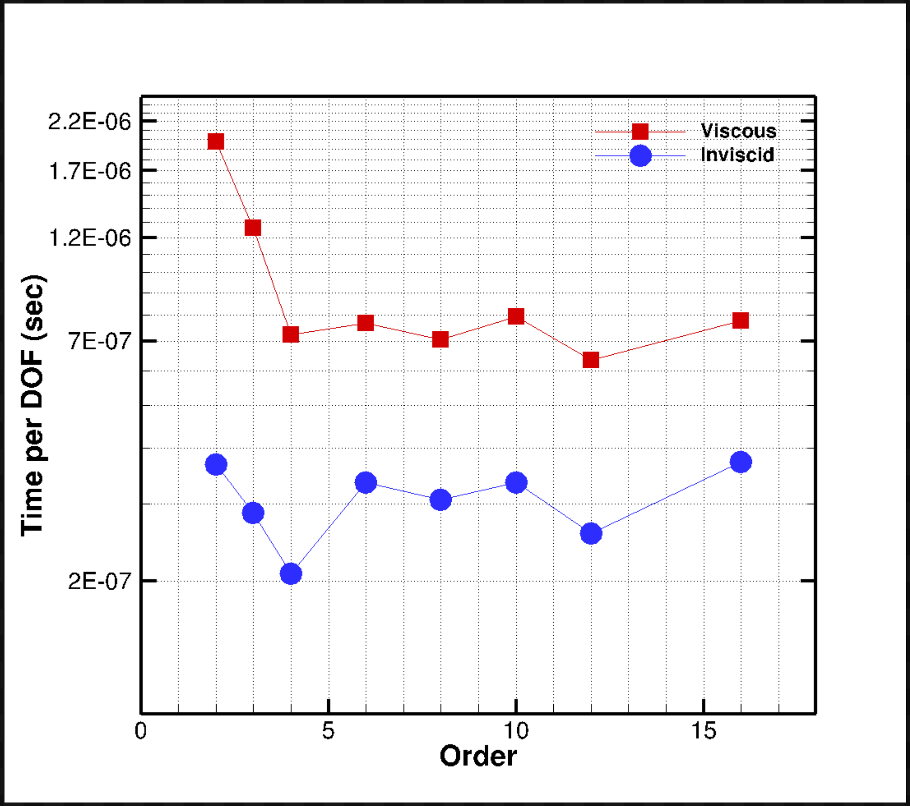

Discontinuous Galerkin vs Finite Difference

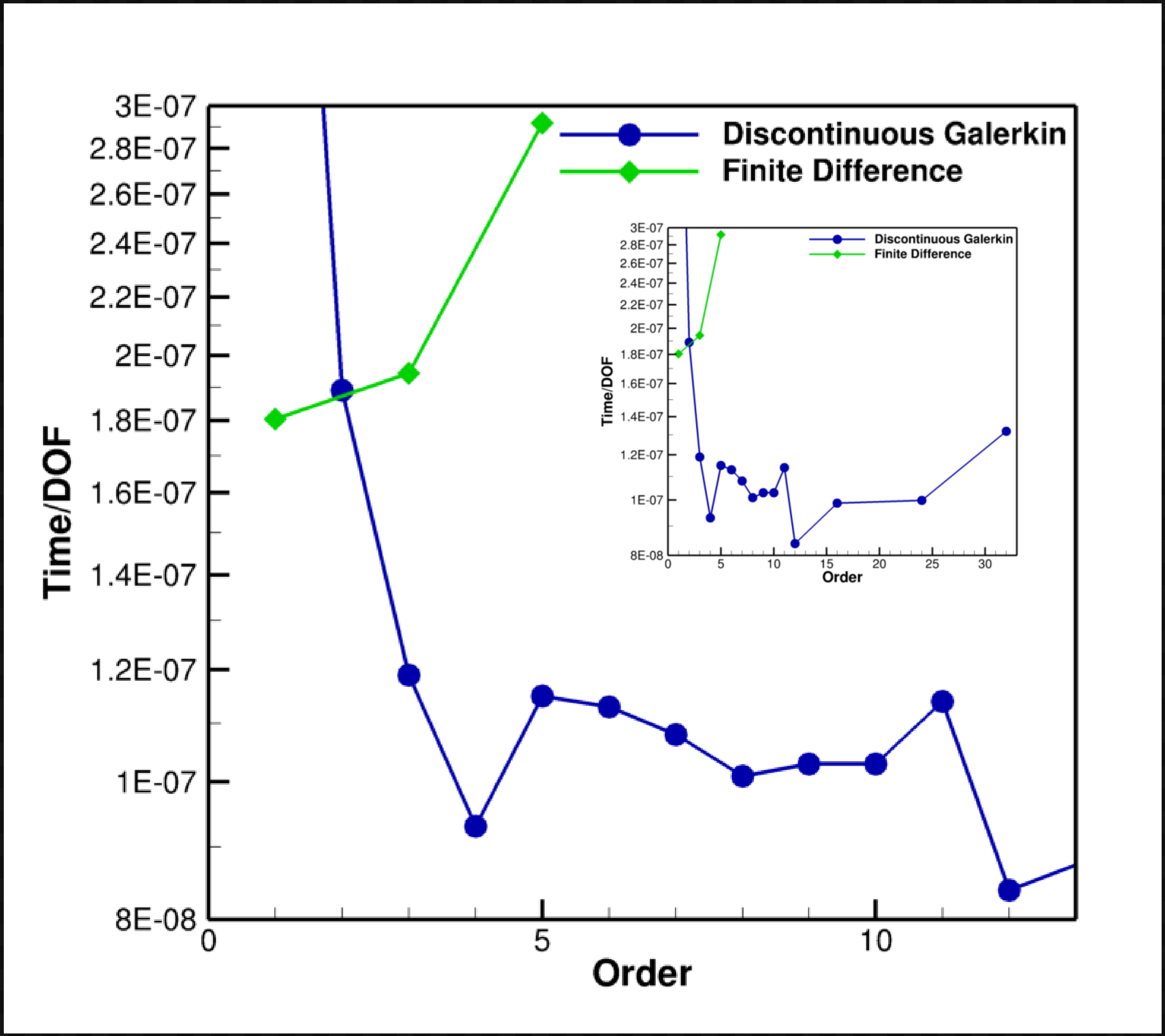

Goals

Develop High-Order CFD Method

- Computationally Efficient
- Parallel Scalable
- Robust
- Multiscale
- Real Applications

Parallel Scalability

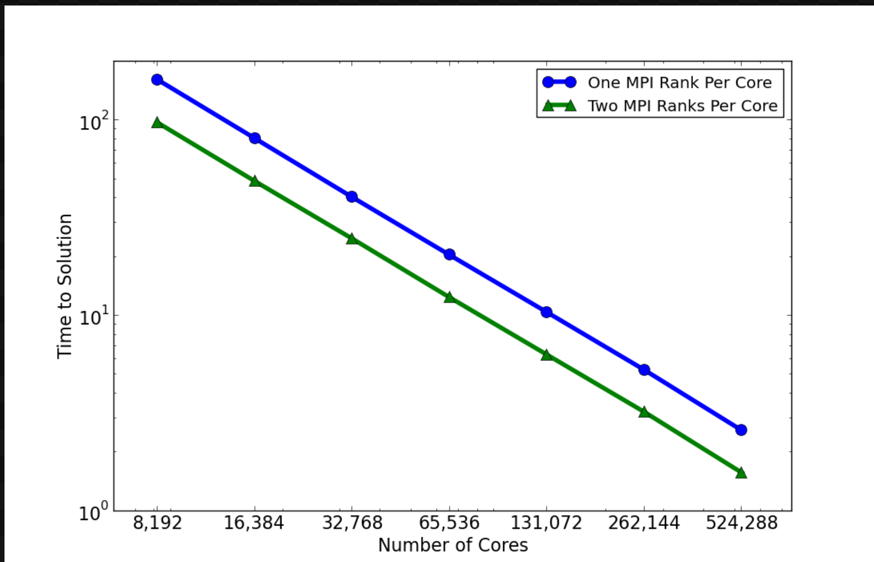

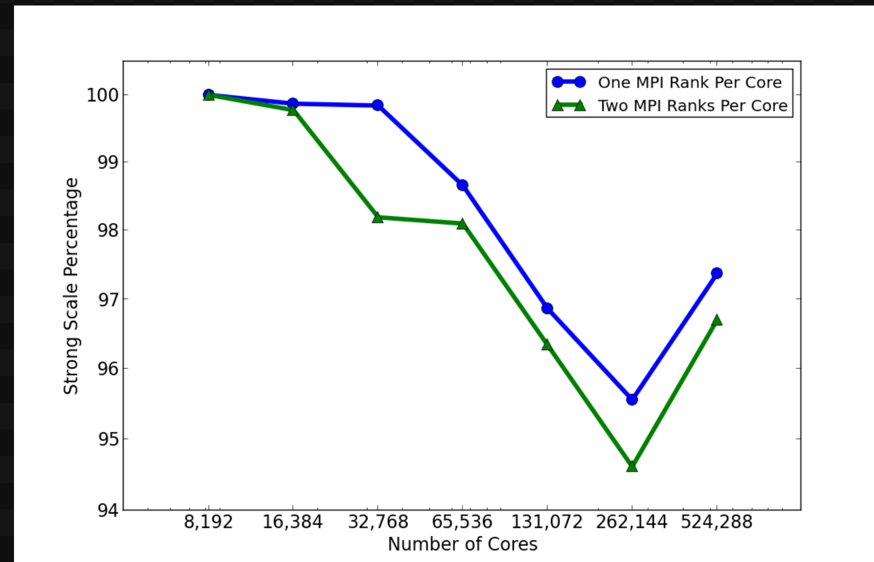

Strong Scaling on ANL Mira

- Taylor-Green Vortex
- Fully periodic
- Mesh: 512 x 512 x 512
- Fifth order: *p* = 4
- 16.8 Billion DOFs
  83.9 Billion unknowns
- 2 MPI ranks per core
  64% faster

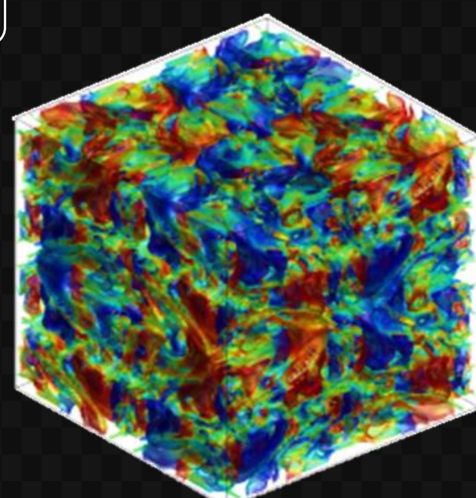

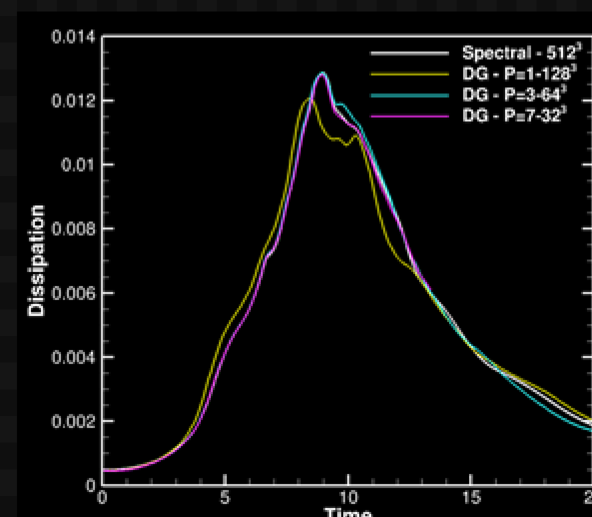

Goals

Develop High-Order CFD Method

Computationally Efficient
Parallel Scalable
Robust
Multiscale
Real Applications

Robustness

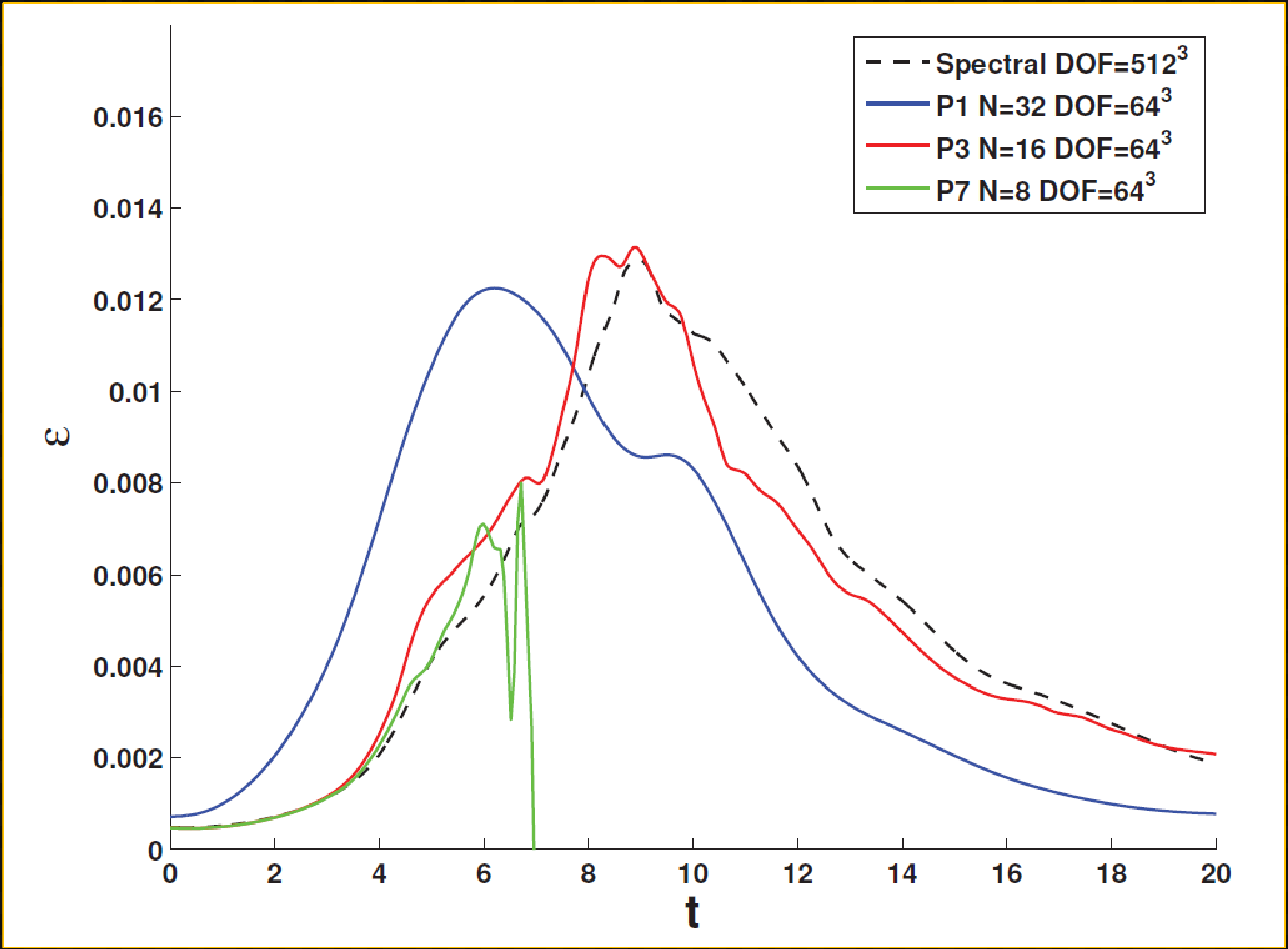
Spectral DOF=512^3
P1 N=32 DOF=64^3
P3 N=16 DOF=64^3
P7 N=8 DOF=64^3
ε
t
0.016
0.014
0.012
0.01
0.008
0.006
0.004
0.002
0
0
2
4
6
8
10
12
14
16
18
20

Robustness

$$\int_{-1}^{1} f(x)dx = \sum_{i=1}^{n} \omega_i f(\xi_i)$$

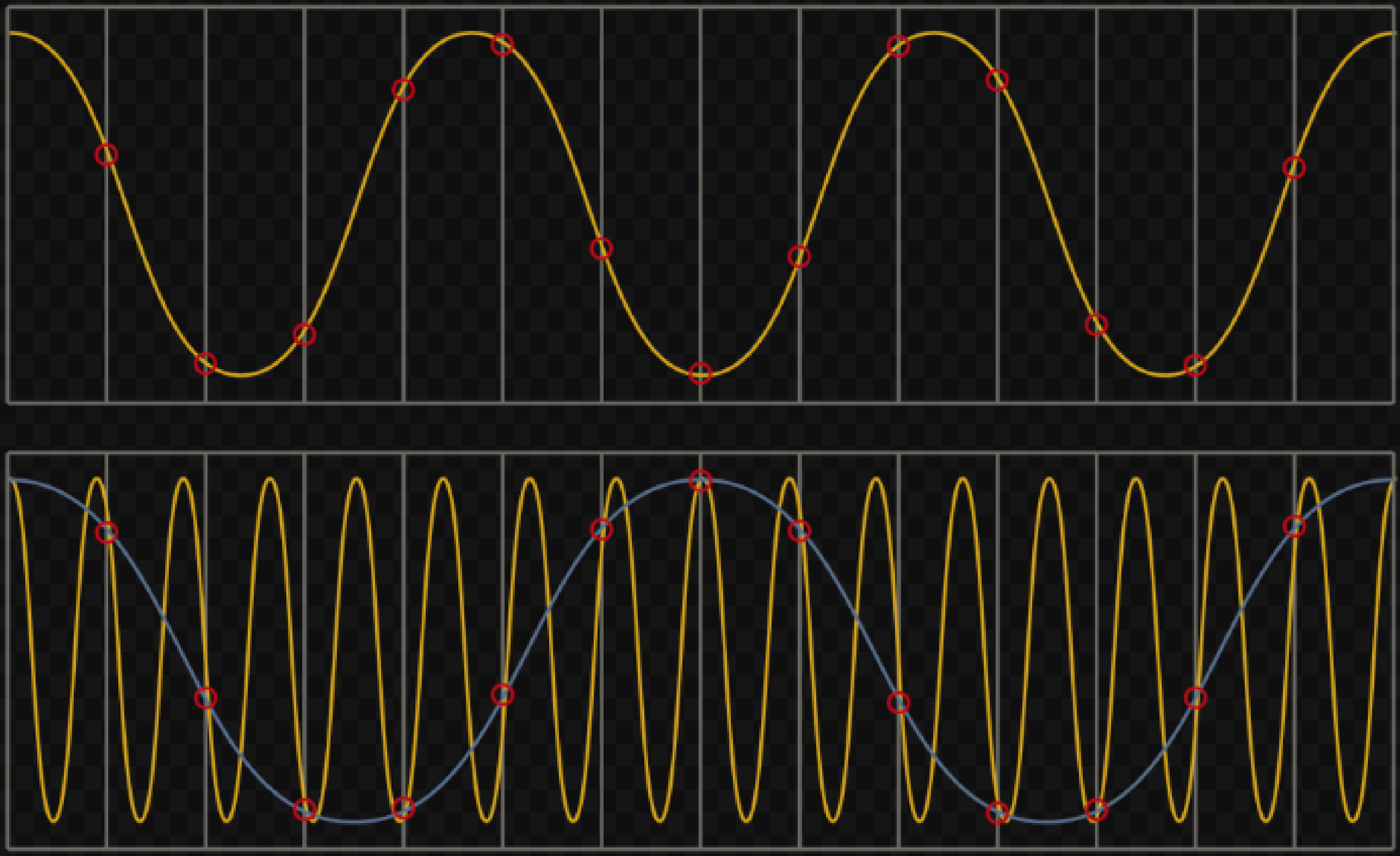

Robustness

$$\int_{-1}^{1} f(x)dx = \sum_{i=1}^{n} \omega_i f(\xi_i)$$

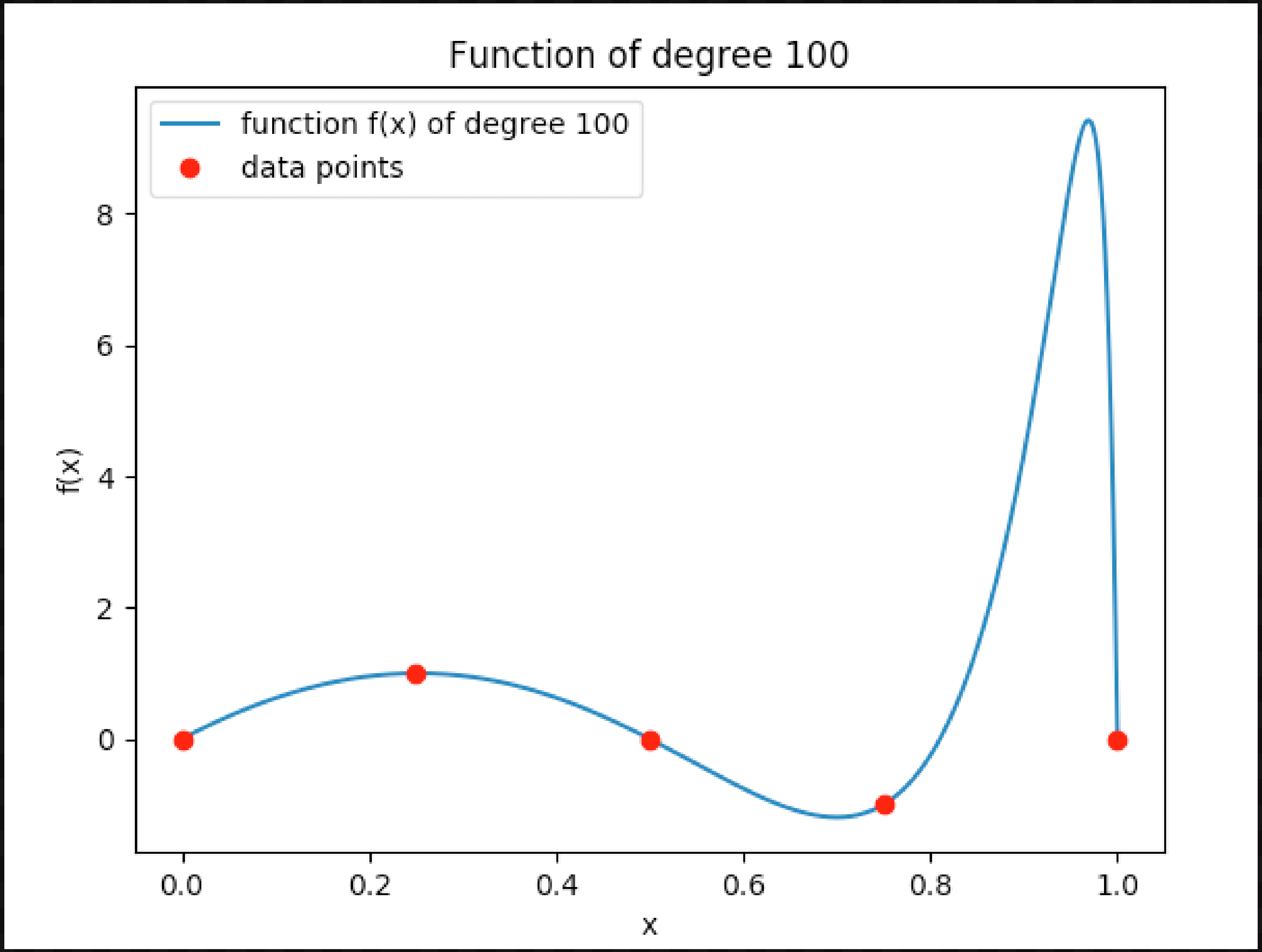

Robustness

Split Formulation with Summation By Parts

Summation By Parts

$$u(x) : [x_L, x_H] \rightarrow \mathbb{R} \qquad v(x) : [x_L, x_H] \rightarrow \mathbb{R}$$

$$\int_{x_L}^{x_H} u(x)\frac{\partial v(x)}{\partial x}\mathrm{d}x = \boxed{u(x)v(x)\Big|_{x_L}^{x_H}} - \boxed{\int_{x_L}^{x_H}\frac{\partial u(x)}{\partial x}v(x)\mathrm{d}x}$$

$$[\mathbf{Q}] := [\mathbf{M}][\mathbf{D}] \quad \text{with} \quad [\mathbf{Q}] + [\mathbf{Q}]^T = [\mathbf{B}] := \mathrm{diag}(-1, 0, \ldots, 0, 1)$$

$$[\mathbf{D}] = [\mathbf{M}]^{-1}[\mathbf{Q}] = \boxed{[\mathbf{M}]^{-1}[\mathbf{B}]} - \boxed{[\mathbf{M}]^{-1}[\mathbf{Q}]^T}$$

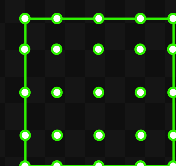

Gauss Lobatto Legendre

$[\mathbf{M}]$ - discrete mass matrix

$[\mathbf{D}]$ - discrete derivative matrix

$$[\mathbf{M}] = \mathrm{diag}(\omega_0, \ldots, \omega_N)$$

$$\boxed{[\mathbf{D}] = D_{ij} = \frac{\mathrm{d}\ell_j(\xi_i)}{\mathrm{d}\xi}}$$

Strong Form Differential

$$\boxed{([\mathbf{M}][\mathbf{D}]) + ([\mathbf{M}][\mathbf{D}])^T = [\mathbf{B}]}$$

Strong Formulation

$$\frac{\partial \mathbf{Q}(\boldsymbol{x},t)}{\partial t} + \vec{\nabla}\cdot\mathbf{F}(\mathbf{Q}(\boldsymbol{x},t)) = 0$$

Finite Element Method

$$\int_{\Omega_k}\left(\frac{\partial \mathbf{Q}}{\partial t} + \boxed{\vec{\nabla}\cdot\mathbf{F}}\right)\psi(\boldsymbol{x})\mathrm{d}\boldsymbol{x} = 0$$

$$\mathbf{R}^{\text{Weak}} = \int_{\Omega_k}\frac{\partial \mathbf{Q}}{\partial t}\psi(\boldsymbol{x})\mathrm{d}\boldsymbol{x}\ \boxed{-\boxed{\int_{\Omega_k}\left(\mathbf{F}\cdot\vec{\nabla}\right)\psi(\boldsymbol{x})\mathrm{d}\boldsymbol{x}} + \int_{\Gamma_k}\left(\mathbf{F}^*\cdot\vec{\mathrm{n}}\right)\psi(\boldsymbol{x}|_{\Gamma_k})\mathrm{d}\Gamma_k} = 0$$

Integrate By Parts Again

$$\mathbf{R}^{\text{Strong}} = \int_{\Omega_k}\frac{\partial \mathbf{Q}}{\partial t}\psi(\boldsymbol{x})\mathrm{d}\boldsymbol{x} + \int_{\Omega_k}\left(\boxed{\vec{\nabla}\mathbf{F}}\cdot\psi(\boldsymbol{x})\right)\mathrm{d}\boldsymbol{x} + \int_{\Gamma_k}\left(\left(\mathbf{F}^*\boxed{-\mathbf{F}}\right)\cdot\vec{\mathrm{n}}\right)\psi(\boldsymbol{x}|_{\Gamma_k})\mathrm{d}\Gamma_k = 0$$

Volume Integral

$$\int_{\Omega_k} \left(\vec{\nabla} \mathbf{F} \cdot \psi(\boldsymbol{x}) \right) \mathrm{d}\boldsymbol{x}$$

$$\int_{\Omega_k} \left(\vec{\nabla} \mathbf{F}(\mathbf{Q}) \cdot \psi(\boldsymbol{x}) \right) \mathrm{d}\boldsymbol{x} = \sum_{d=1}^{3} \int_{E} \boxed{\frac{\partial \mathcal{F}^d(\mathbf{Q}(\boldsymbol{\xi}))}{\partial \xi^d}} \psi(\boldsymbol{\xi}) \mathrm{d}\boldsymbol{\xi}$$

$$\frac{\partial \mathcal{F}^d(\mathbf{Q}(\boldsymbol{\xi}))}{\partial \xi^d} = \sum_{n,n,l=1}^{N} \tilde{\mathcal{F}}^d_{mnl} \frac{\partial \left[\ell_m(\xi^1) \ell_n(\xi^2) \ell_l(\xi^3) \right]}{\partial \xi^d}$$

Strong Formulation Volume Integral:

$$\int_{\Omega_k} \left(\vec{\nabla} \mathbf{F}(\mathbf{Q}) \cdot \psi(\boldsymbol{x}) \right) \mathrm{d}\boldsymbol{x} = \omega_i \omega_j \omega_k \sum_{m=1}^{N} \overline{\overline{D}}_{im} \tilde{\mathcal{F}}^1_{mjk} + \omega_i \omega_j \omega_k \sum_{n=1}^{N} \overline{\overline{D}}_{jn} \tilde{\mathcal{F}}^2_{ink} + \omega_i \omega_j \omega_k \sum_{l=1}^{N} \overline{\overline{D}}_{kl} \tilde{\mathcal{F}}^3_{ijl}$$

$$\overline{\overline{D}}_{ij} = \frac{\mathrm{d}\ell_j(\xi_i)}{\mathrm{d}\xi}, \qquad i, j = 0, \ldots, N$$

Split Form

$$J\frac{\partial \tilde{\mathbf{Q}}}{\partial t} + \tilde{\vec{\mathcal{L}}}_X\left(\mathbf{Q}\right) + \tilde{\vec{\mathcal{L}}}_Y\left(\mathbf{Q}\right) + \tilde{\vec{\mathcal{L}}}_Z\left(\mathbf{Q}\right) = 0$$

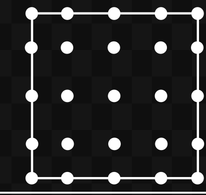

Gauss Lobatto Legendre

$$\left(\tilde{\vec{\mathcal{L}}}_X\left(\mathbf{Q}\right)\right)_{i,j,k} \approx \frac{1}{\omega_i}\left(\delta_{iN}\left[\tilde{\mathcal{F}}^* - \tilde{\mathcal{F}}\right]_{Njk} - \delta_{i1}\left[\tilde{\mathcal{F}}^* - \tilde{\mathcal{F}}\right]_{1jk}\right) + \sum_{m=1}^{N} \mathbf{D}_{im}(\tilde{\mathcal{F}})_{mjk}$$

$$\left(\tilde{\vec{\mathcal{L}}}_Y\left(\mathbf{Q}\right)\right)_{i,j,k} \approx \frac{1}{\omega_j}\left(\delta_{jN}\left[\tilde{\mathcal{G}}^* - \tilde{\mathcal{G}}\right]_{iNk} - \delta_{j1}\left[\tilde{\mathcal{G}}^* - \tilde{\mathcal{G}}\right]_{i1k}\right) + \sum_{m=1}^{N} \mathbf{D}_{jm}(\tilde{\mathcal{G}})_{imk}$$

$$\left(\tilde{\vec{\mathcal{L}}}_Z\left(\mathbf{Q}\right)\right)_{i,j,k} \approx \frac{1}{\omega_k}\left(\delta_{kN}\left[\tilde{\mathcal{H}}^* - \tilde{\mathcal{H}}\right]_{ijN} - \delta_{k1}\left[\tilde{\mathcal{H}}^* - \tilde{\mathcal{H}}\right]_{ij1}\right) + \sum_{m=1}^{N} \mathbf{D}_{km}(\tilde{\mathcal{H}})_{ijm}$$

$$\sum_{m=1}^{N} \mathbf{D}_{im}(\tilde{\mathcal{F}})_{mjk} \approx \sum_{m=1}^{N} 2\mathbf{D}_{im} F^{\#}(\mathbf{Q}_{ijk}, \mathbf{Q}_{mjk})$$

Interpreted as sub-cell volume differencing operator $[\mathbf{D}]$

Flux Splitting

$$\sum_{m=1}^{N} \mathbf{D}_{im}(\tilde{\mathcal{F}})_{mjk} \approx \sum_{m=1}^{N} 2\mathbf{D}_{im} F^{\#}(\mathbf{Q}_{ijk}, \mathbf{Q}_{mjk})$$

$$\{\!\{a\}\!\} := \frac{1}{2}(a_1 + a_2)$$

$$F^{\#}(\mathbf{Q}_1, \mathbf{Q}_2) = \{\!\{\rho\}\!\}\{\!\{u\}\!\} = \frac{1}{2}(\rho_1 + \rho_2) \cdot \frac{1}{2}(u_1 + u_2)$$

Strong Form

$$F^{\#,\text{standard}}(\mathbf{Q}_{ijk}, \mathbf{Q}_{mjk}) = \begin{bmatrix} \{\!\{\rho u\}\!\} \\ \{\!\{\rho u u + p\}\!\} \\ \{\!\{\rho u v\}\!\} \\ \{\!\{\rho u w\}\!\} \\ \{\!\{\rho u e + p u\}\!\} \end{bmatrix}$$

Kennedy & Gruber

$$F^{\#,\text{KG}}(\mathbf{Q}_{ijk}, \mathbf{Q}_{mjk}) = \begin{bmatrix} \{\!\{\rho\}\!\}\{\!\{u\}\!\} \\ \{\!\{\rho\}\!\}\{\!\{u\}\!\}\{\!\{u\}\!\} + \{\!\{p\}\!\} \\ \{\!\{\rho\}\!\}\{\!\{u\}\!\}\{\!\{v\}\!\} \\ \{\!\{\rho\}\!\}\{\!\{u\}\!\}\{\!\{w\}\!\} \\ \{\!\{\rho\}\!\}\{\!\{u\}\!\}\{\!\{e\}\!\} + \{\!\{p\}\!\}\{\!\{u\}\!\} \end{bmatrix}$$

Pirozzoli

$$F^{\#,\text{PZ}}(\mathbf{Q}_{ijk}, \mathbf{Q}_{mjk}) = \begin{bmatrix} \{\!\{\rho\}\!\}\{\!\{u\}\!\} \\ \{\!\{\rho\}\!\}\{\!\{u\}\!\}\{\!\{u\}\!\} + \{\!\{p\}\!\} \\ \{\!\{\rho\}\!\}\{\!\{u\}\!\}\{\!\{v\}\!\} \\ \{\!\{\rho\}\!\}\{\!\{u\}\!\}\{\!\{w\}\!\} \\ \{\!\{\rho\}\!\}\{\!\{u\}\!\}\{\!\{h\}\!\} \end{bmatrix}$$

Surface Flux Consistency

$$\mathbf{R}^{\text{Strong}} = \int_{\Omega_k} \frac{\partial \mathbf{Q}}{\partial t} \psi(\boldsymbol{x}) \mathrm{d}\boldsymbol{x} + \int_{\Omega_k} \left(\vec{\nabla} \mathbf{F} \cdot \psi(\boldsymbol{x}) \right) \mathrm{d}\boldsymbol{x} + \int_{\Gamma_k} \left(\left(\boxed{\mathbf{F}^*} - \mathbf{F} \right) \cdot \vec{\mathrm{n}} \right) \psi(\boldsymbol{x}|_{\Gamma_k}) \mathrm{d}\Gamma_k = 0$$

$$\boxed{F^* \left(\mathbf{Q}_-, \mathbf{Q}_+ \right) := F^{\text{Symmetric}} \left(\mathbf{Q}_-, \mathbf{Q}_+ \right) - F^{\text{Stab}} \left(\mathbf{Q}_-, \mathbf{Q}_+ \right)}$$

$$\boxed{F^* \left(\mathbf{Q}_-, \mathbf{Q}_+ \right) = \boxed{F^{\#}} \left(\mathbf{Q}_-, \mathbf{Q}_+ \right) - F^{\text{Stab}} \left(\mathbf{Q}_-, \mathbf{Q}_+ \right)}$$

Kennedy & Gruber

$$F^{\#,\mathbf{KG}} \left(\mathbf{Q}_{ijk}, \mathbf{Q}_{mjk} \right) = \begin{bmatrix} \{\!\{\rho\}\!\}\{\!\{u\}\!\} \\ \{\!\{\rho\}\!\}\{\!\{u\}\!\}\{\!\{u\}\!\} + \{\!\{p\}\!\} \\ \{\!\{\rho\}\!\}\{\!\{u\}\!\}\{\!\{v\}\!\} \\ \{\!\{\rho\}\!\}\{\!\{u\}\!\}\{\!\{w\}\!\} \\ \{\!\{\rho\}\!\}\{\!\{u\}\!\}\{\!\{e\}\!\} + \{\!\{p\}\!\}\{\!\{u\}\!\} \end{bmatrix}$$

Robustness Results

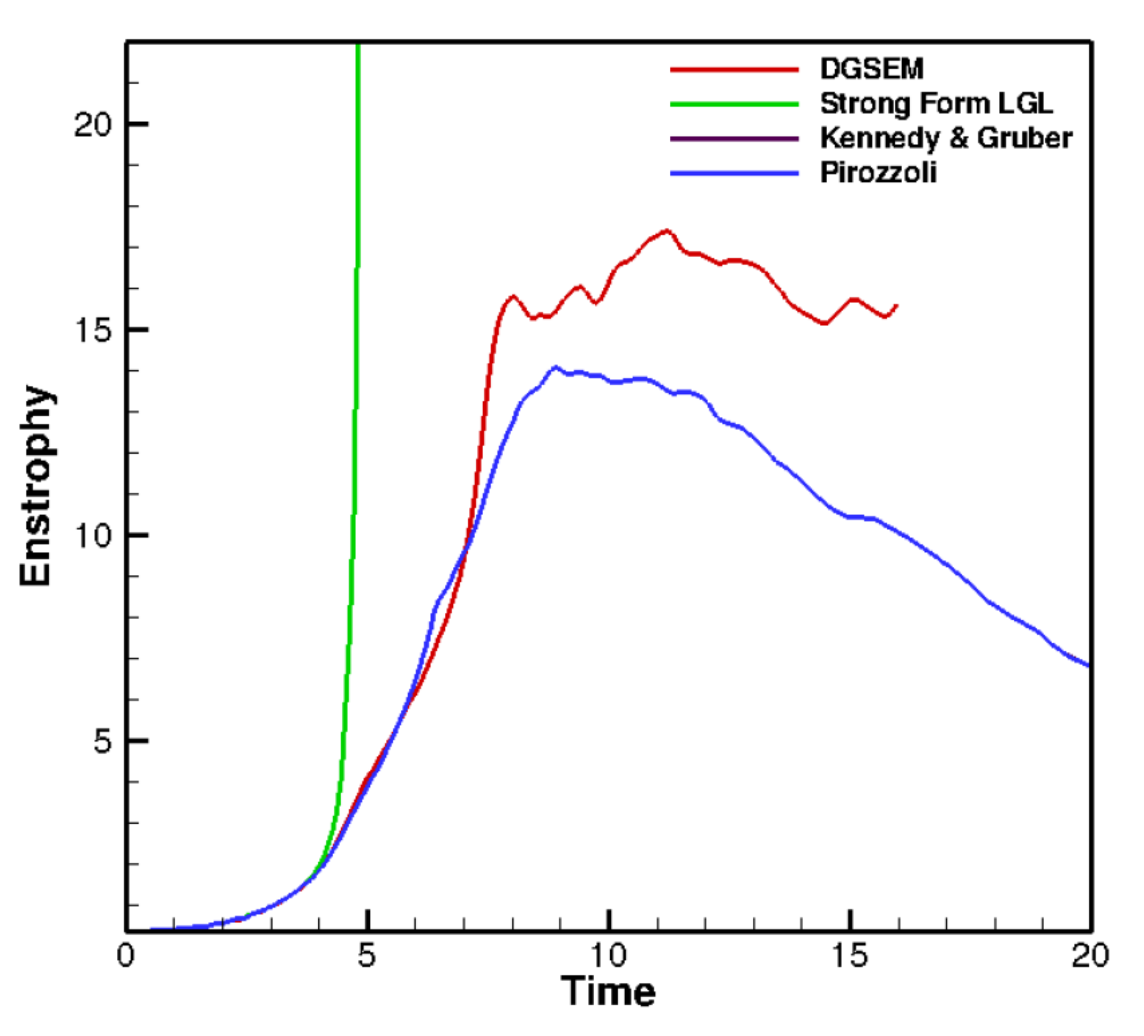

16 Fourth-Order Elements

Goals

Develop High-Order CFD Method

- Computationally Efficient
- Parallel Scalable
- Robust
- Multiscale
- Real Applications

Multiscale Problems

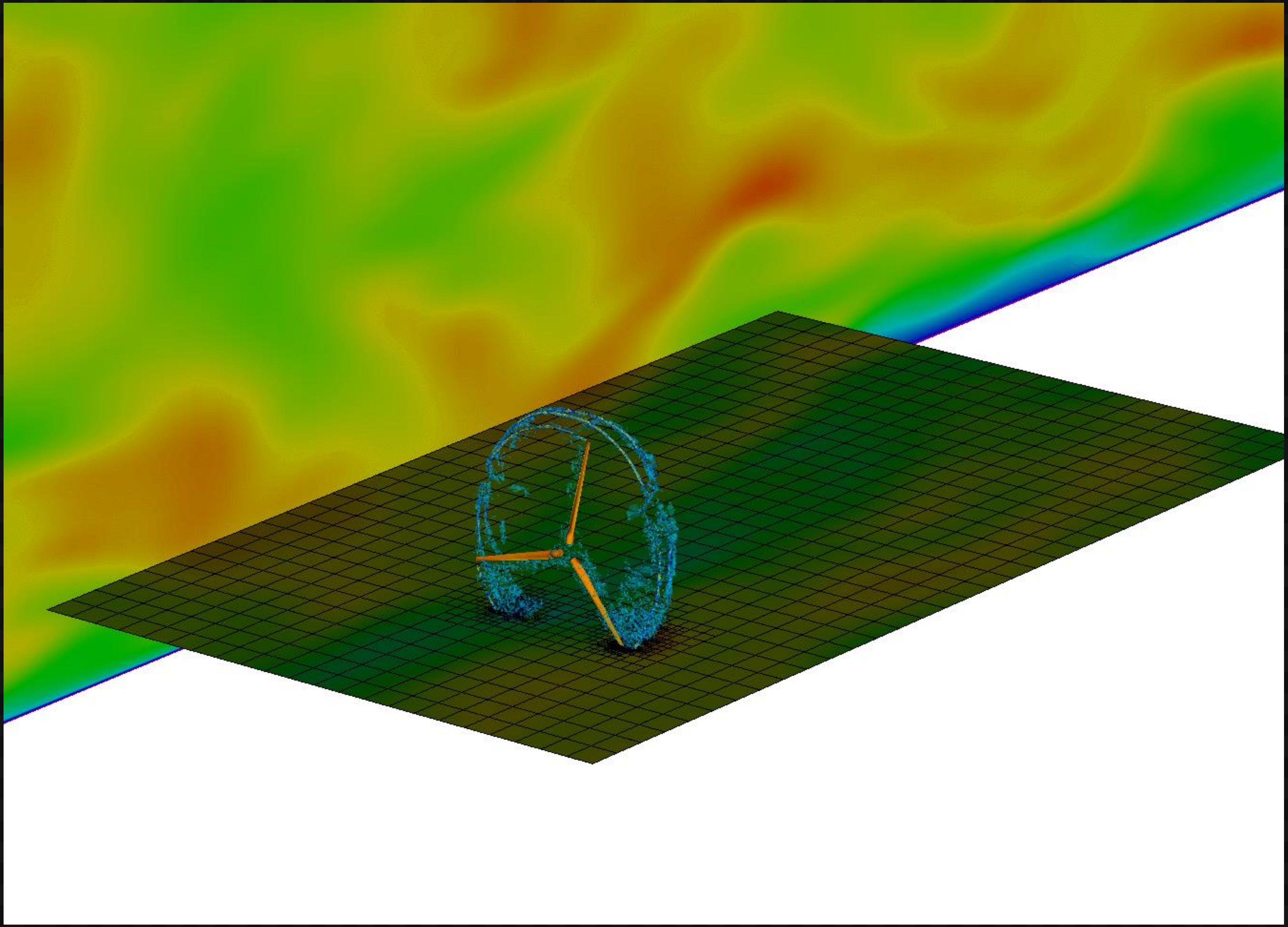

Adaptive Mesh Refinement

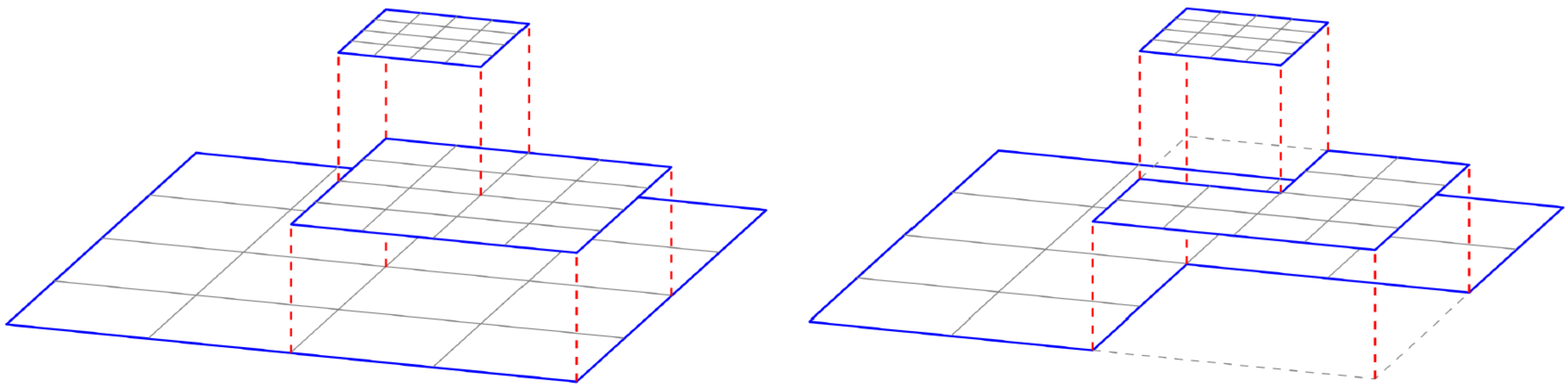

(a) patch-based AMR (b) octree-based AMR

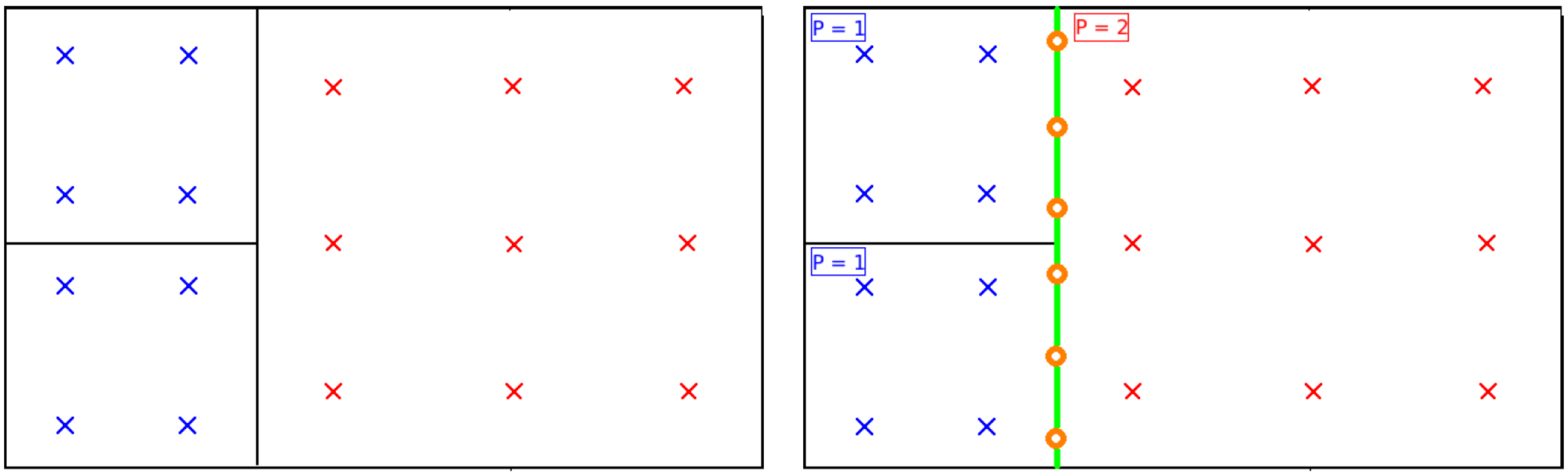

(a) hanging element face (b) mortar element interface

AMR Operators

Projection/Refine

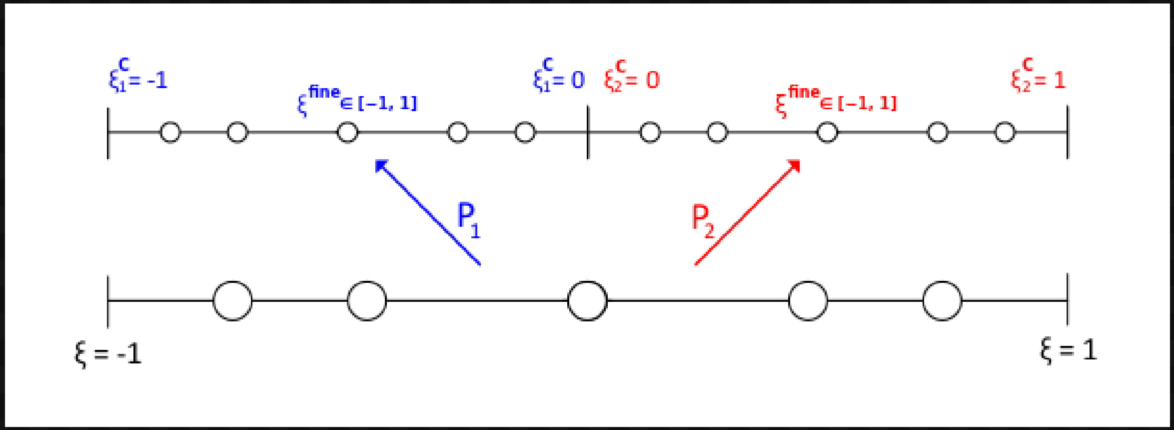

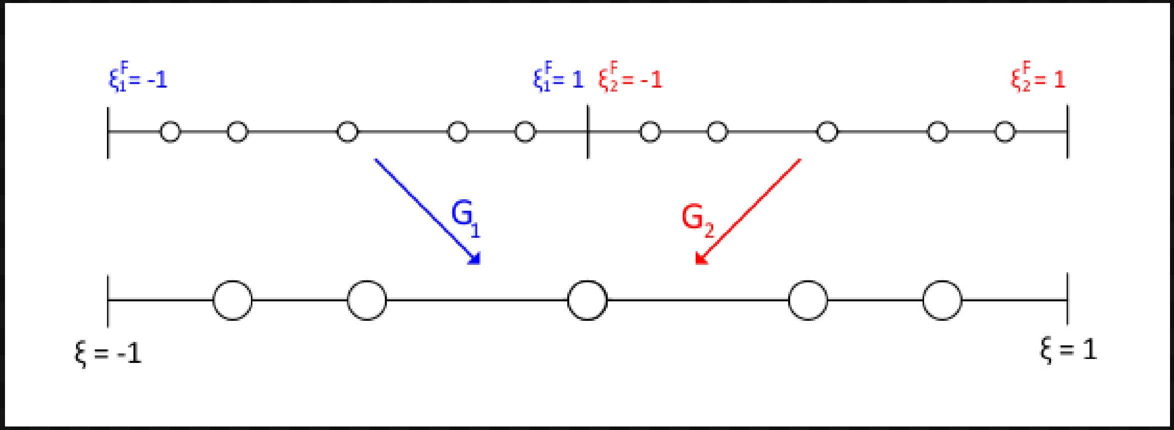

Restriction/Coarsen

COLLEGE OF ENGINEERING & APPLIED SCIENCE
UNIVERSITY of WYOMING

Verification

2L1P

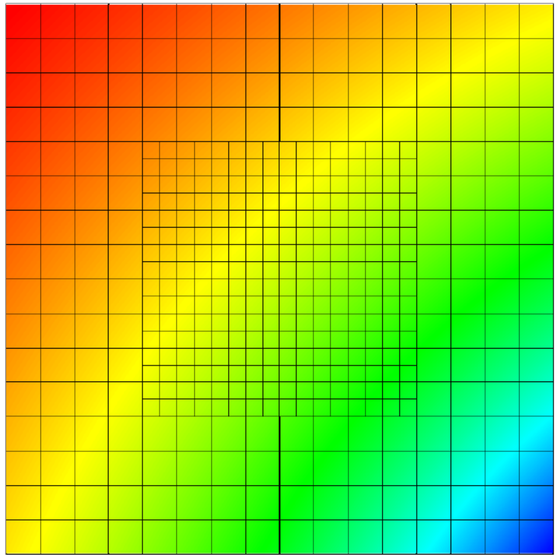

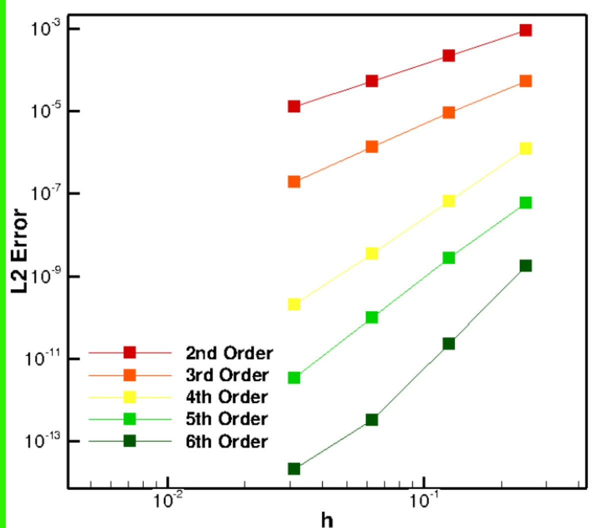

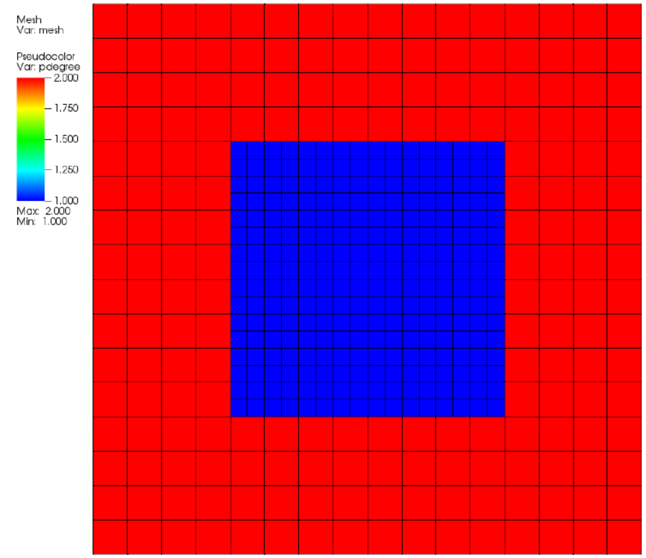

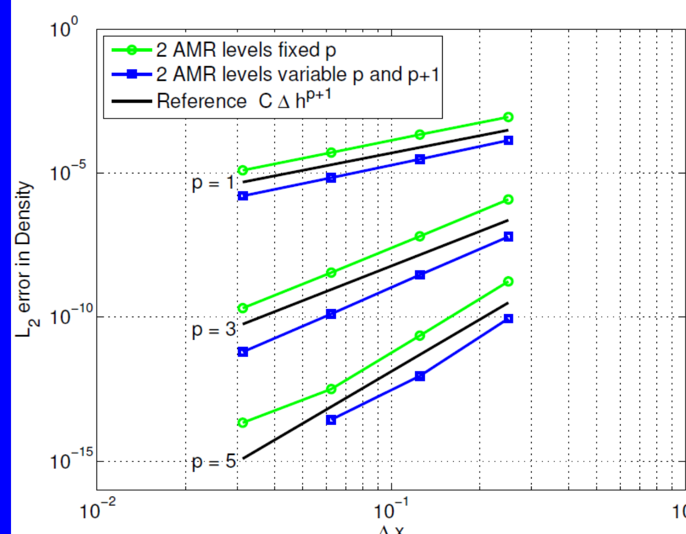

2L2P

Feature-Based Tagging

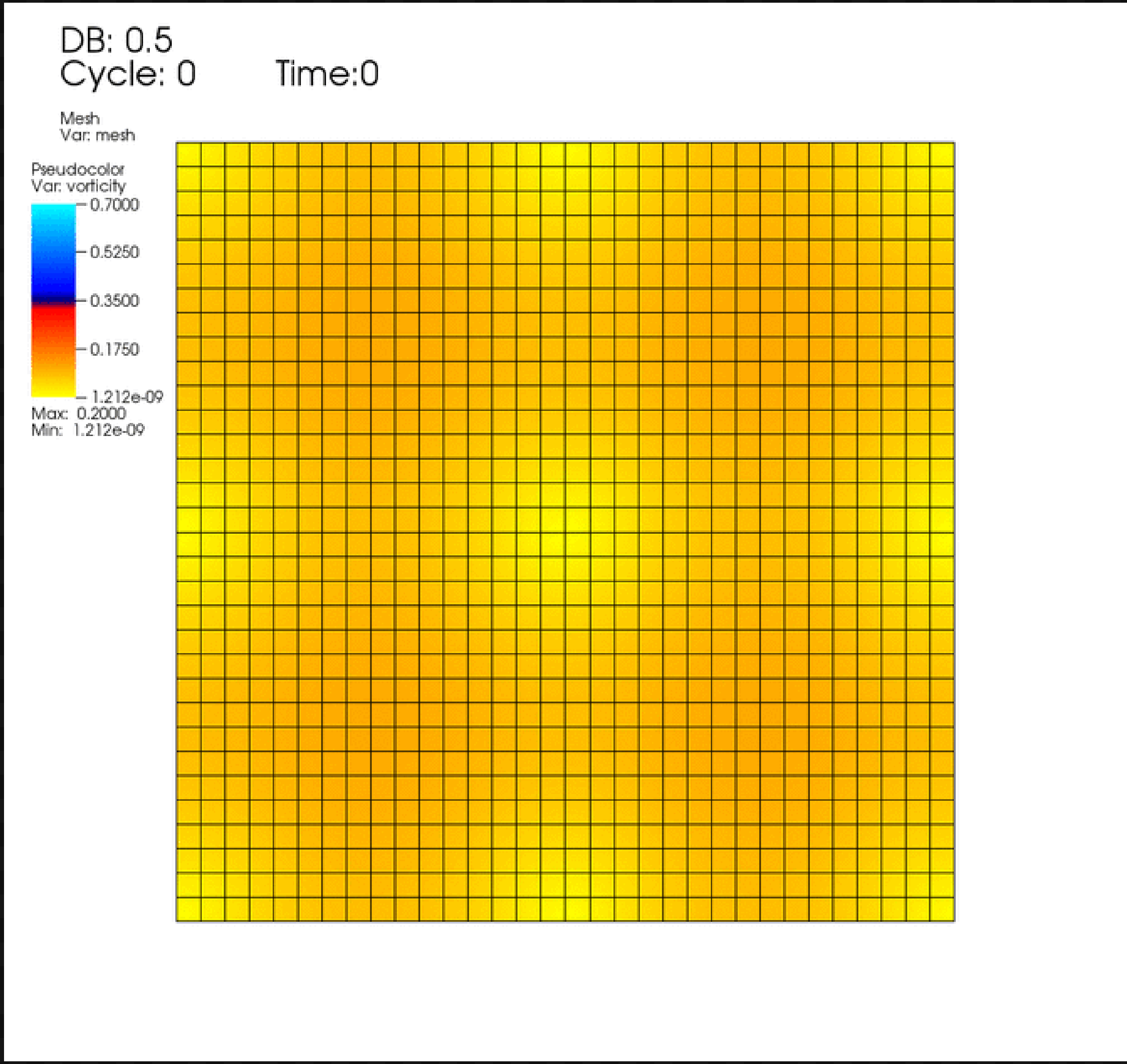

hp-Adaption

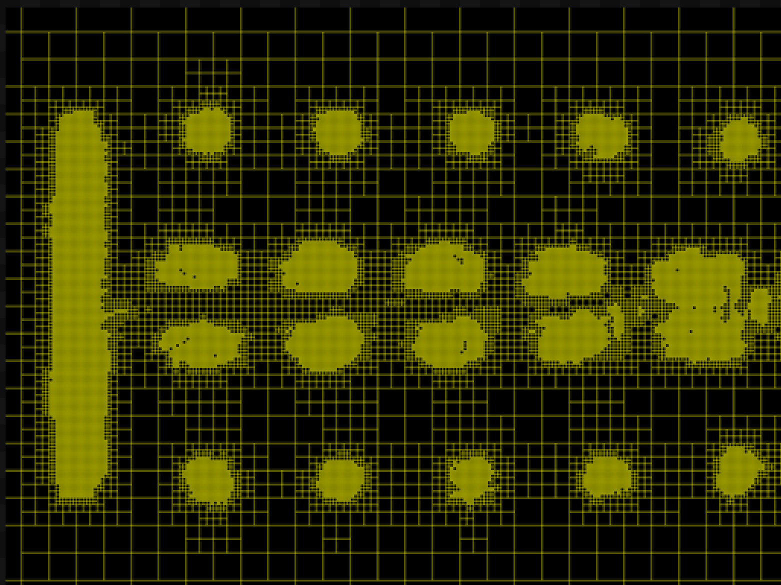

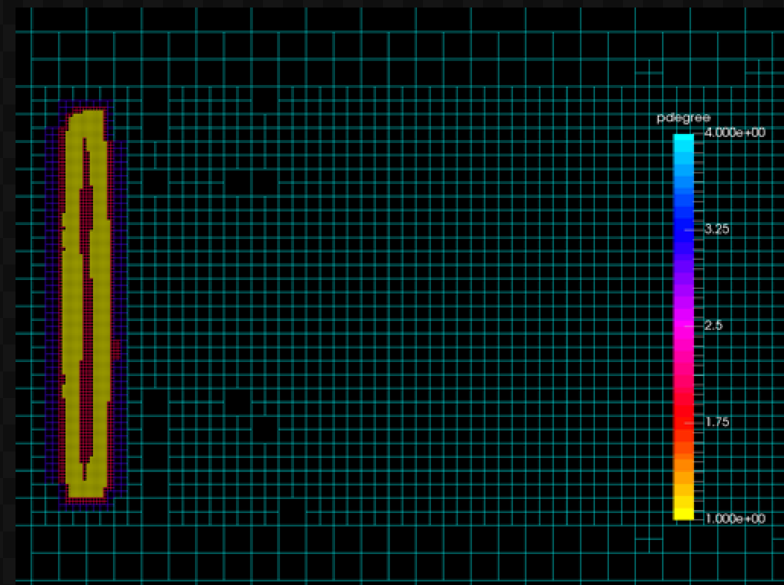

p=1
2nd-order

p=1 - 4
2nd- to 5th-order

hp-Adaption

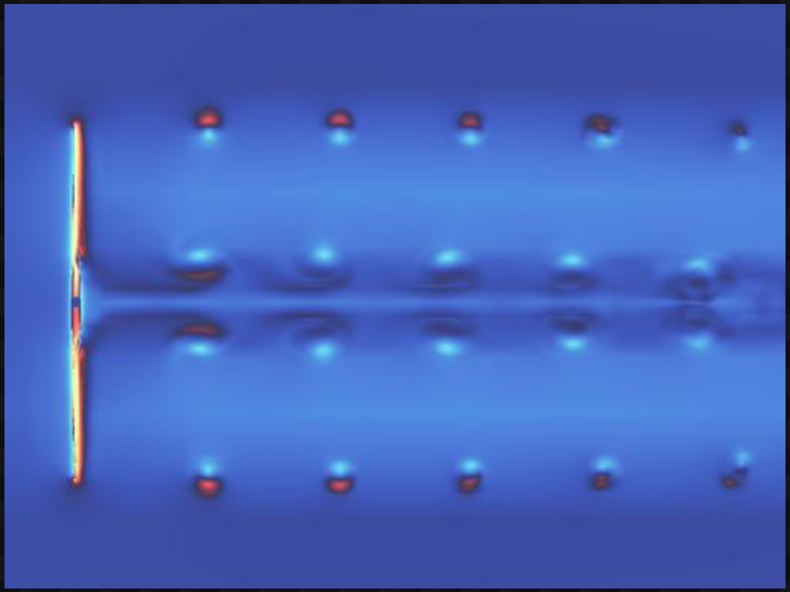

p=1
2^{nd}-order

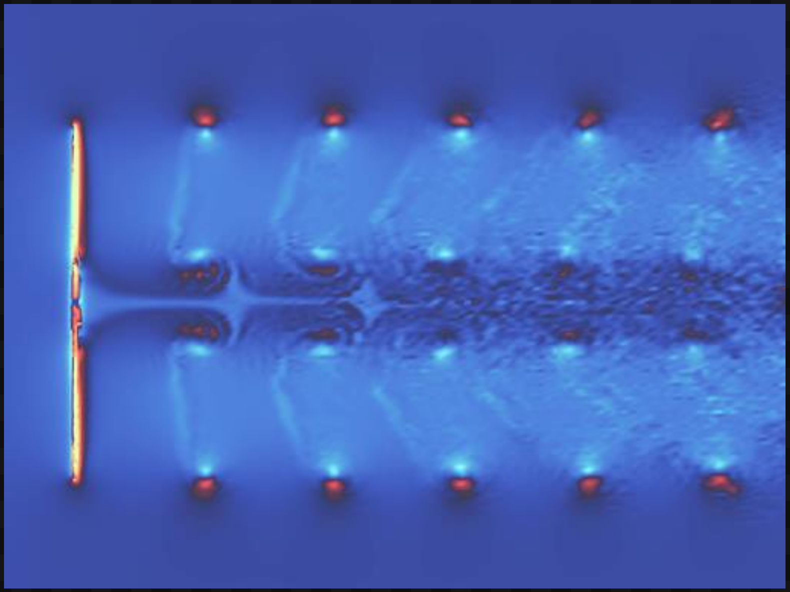

p=1 - 4
2^{nd}- to 5^{th}-order

Goals

Develop High-Order CFD Method

- Computationally Efficient
- Parallel Scalable
- Robust
- Multiscale
- Real Applications

Overall Strategy

Wyoming **W**ind and **A**erospace **A**pplication **K**omputation **E**nvironment

- Multidisciplinary
  - CFD
  - Atmospheric turbulence
  - Structural dynamics
  - Controls
  - Acoustics
- Multi Mesh-Multi Solver Paradigm
  - Near-body unstructured mesh with sub-layer resolution
  - Off-body structured/Cartesian high-order discontinuous Galerkin solver
  - Adaptive mesh refinement (p4est)
  - Overset meshes (TIOGA)
- HPC
  - Scalability
  - In-situ visualization/data reduction

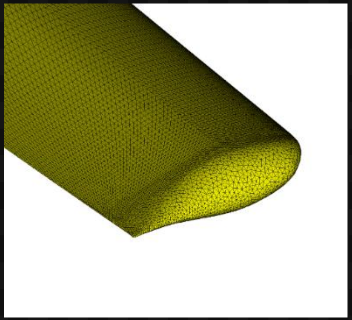

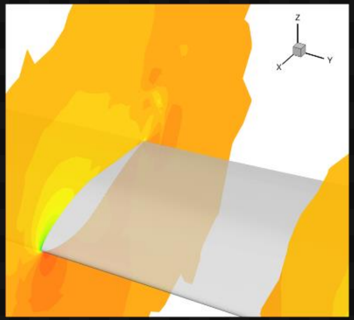

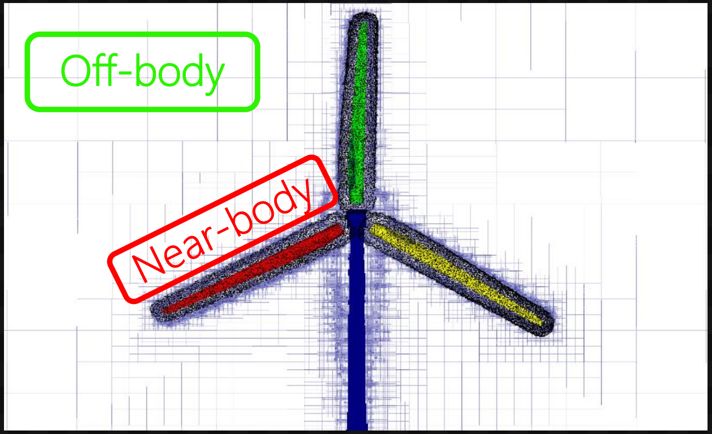

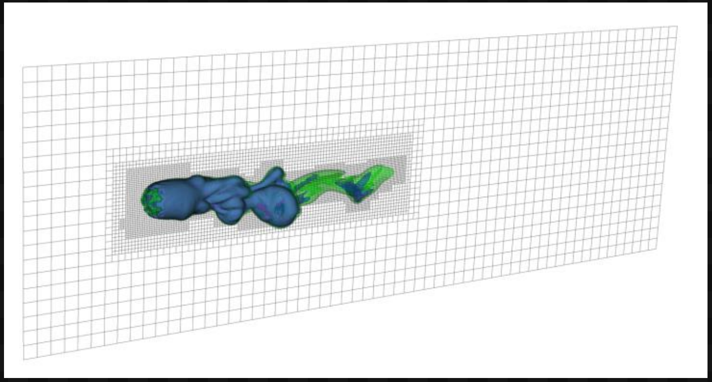

Computational Framework

W^2A^2KE3D

Solvers

NSU3D

- High-fidelity viscous RANS analysis
  - Resolves thin boundary layer to wall
  - O(10^{-6}) normal spacing
  - Suite of turbulence models available
- Stiff discrete equations to solve
  - Implicit line solver
  - Agglomeration Multigrid acceleration
- High accuracy objective
  - 1 drag count
- Unstructured mixed element grids for complex geometries
- Validated through AIAA Drag/High-Lift Prediction Workshops

DG4est

- High-order discretization
  - Discontinuous Galerkin method
    - Split form w/ summation-by-parts
- Adaptive mesh refinement
  - p4est AMR framework
  - Dynamic adaption
  - *hp*-refinement strategy

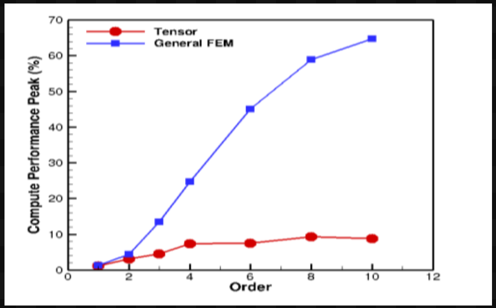

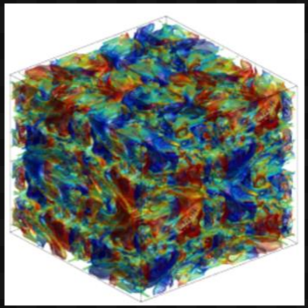

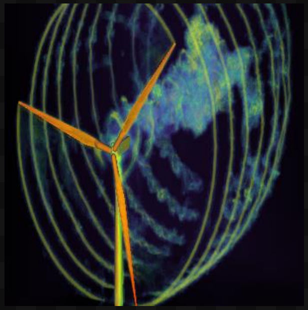

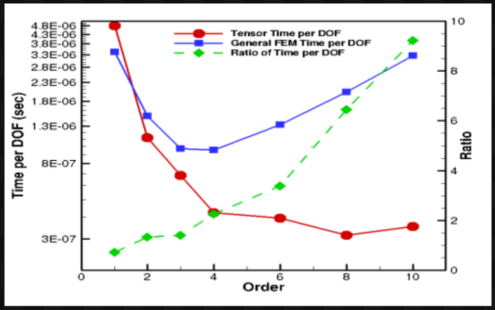

SCIENTIFIC SIMULATIONS

Motivation
Governing Equations
Discretization
Goals
Results
Conclusions
Future Work

Wind Energy

- Simulation-based analysis, design and optimization and for large wind plant installations
  - Largest gains to be had at the wind plant scale
  - 20% to 30% installed losses
  - Optimization of siting
  - Operational techniques for increased output and life
  - Development of control techniques at high fidelity
- Blade-resolved models enable:
  - Accurate prediction of flow separation/stalling
  - Effect on blade loads, wake structure
  - Interaction with atmospheric turbulence structures
  - Incorporation of additional effects
    - Icing, contamination (transition)
    - Acoustics (FWH methods)

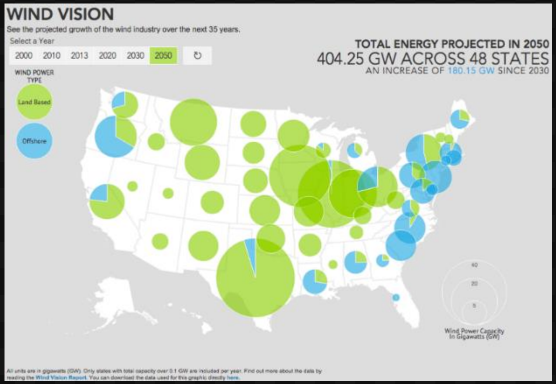

EXASCALE COMPUTING PROJECT

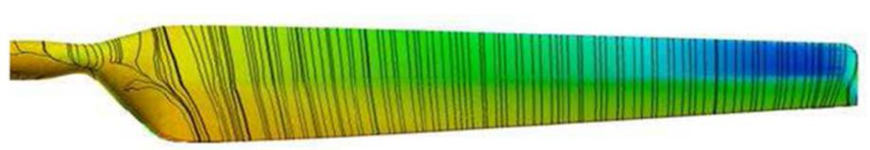
(a) $V = 7m\ s^{-1}$

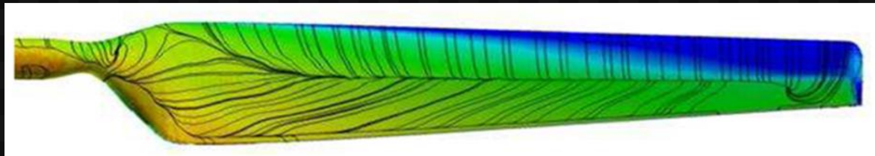
(b) $V = 10m\ s^{-1}$

Results

- Mesh Resolution Study
  - NREL-5MW
- Single Long Run-Time Study
  - NREL WindPACT-1.5MW
- Single Baseline Turbine Validation
  - Siemens SWT-2.3-93
- Wind Farm Simulation
  - Lillgrund 48 Wind Turbine Farm

Results

Mesh Resolution Study

NREL-5MW

Single Long Run-Time Study

NREL WindPACT-1.5MW

Single Baseline Turbine Validation

Siemens SWT-2.3-93

Wind Farm Simulation

Lillgrund 48 Wind Turbine Farm

NREL 5MW

Mesh	Mesh Points
Coarse*	474,383
Coarse	360,148
Medium	927,701
Fine	2,873,862

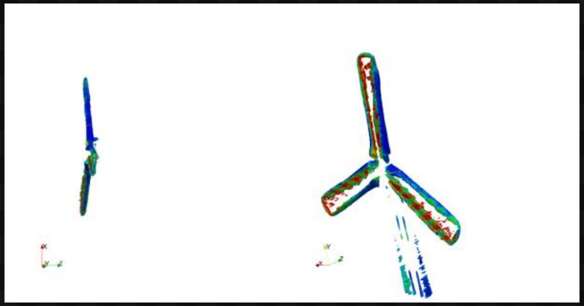

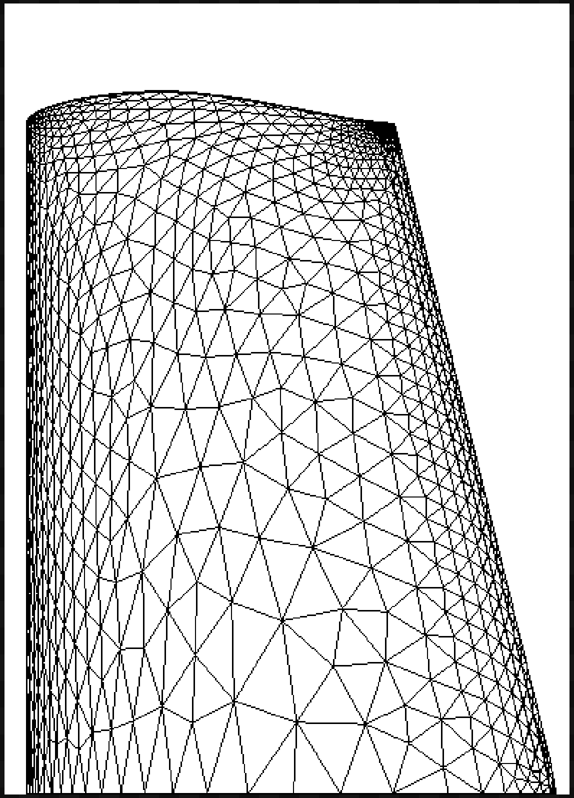

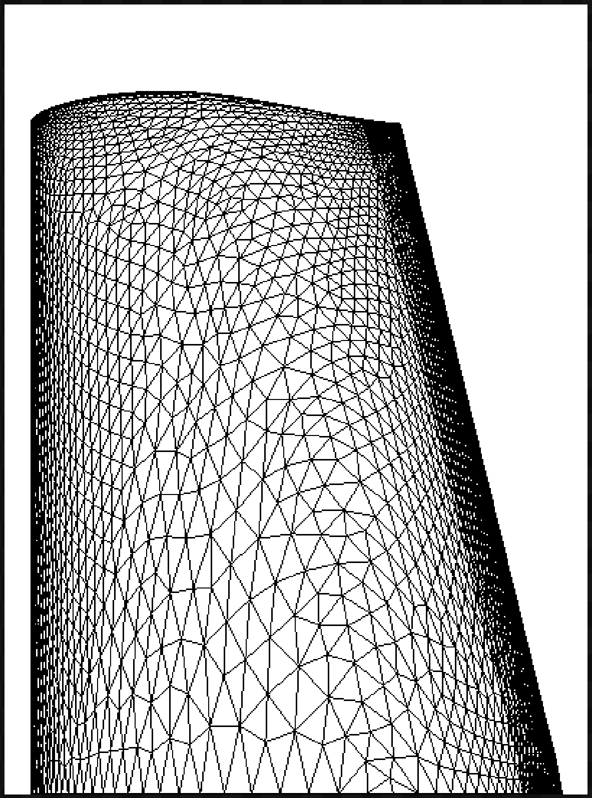

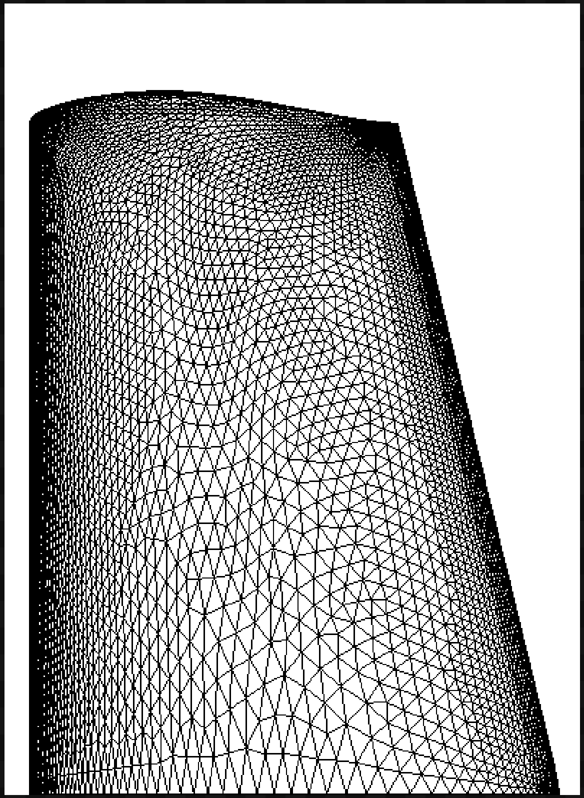

AIAA Paper 2017-3958

NREL 5MW

Mesh Resolution Study

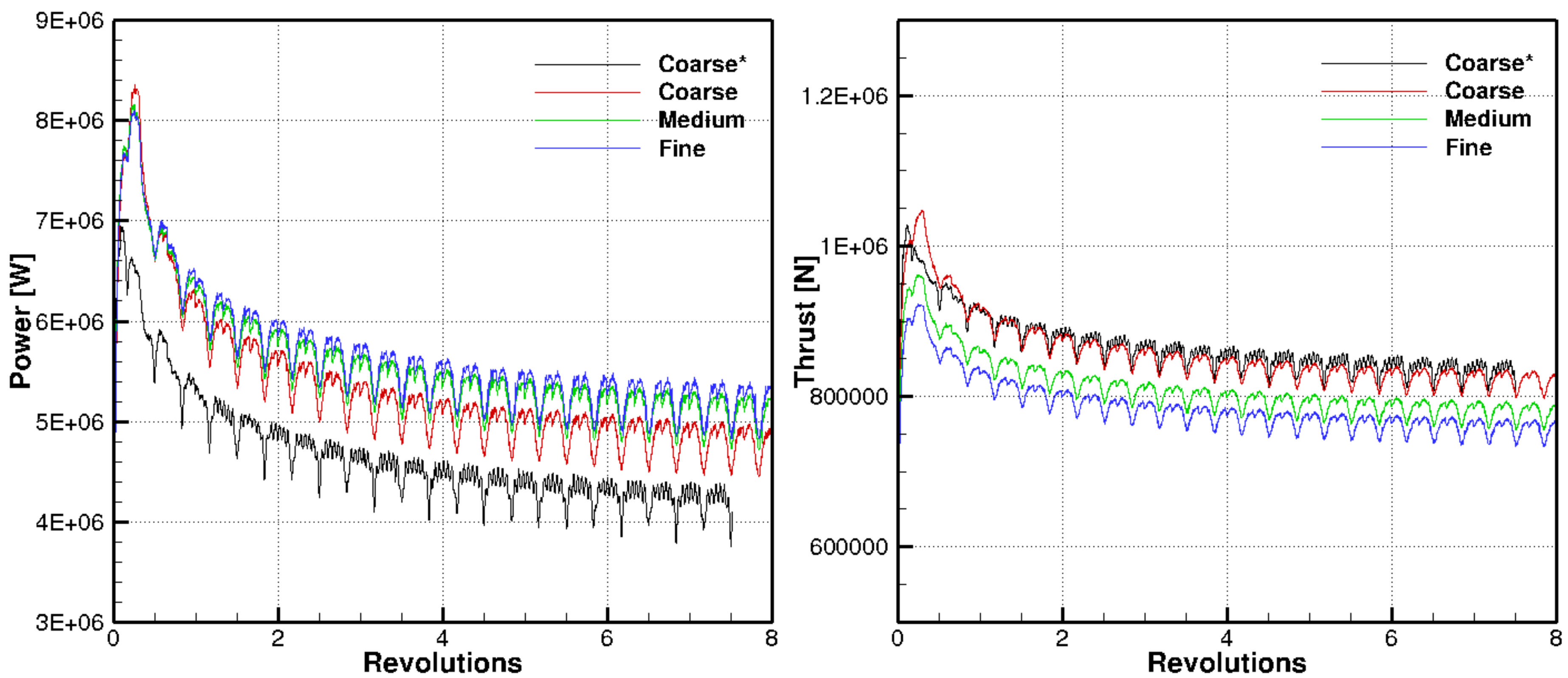

AIAA Paper 2017-3958

NREL 5MW

Inflow Velocity Sweep

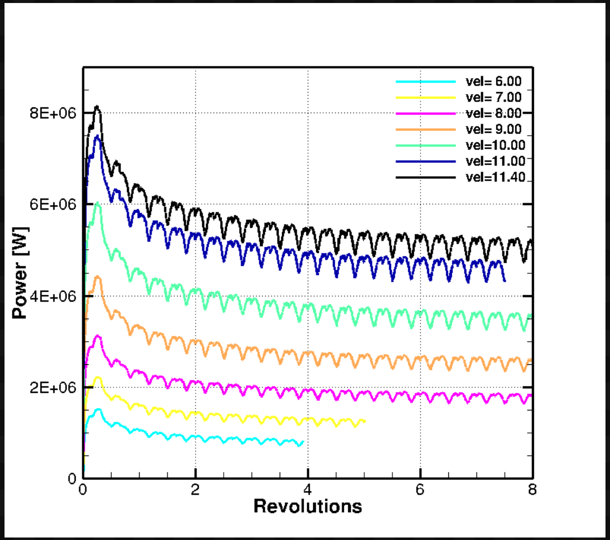

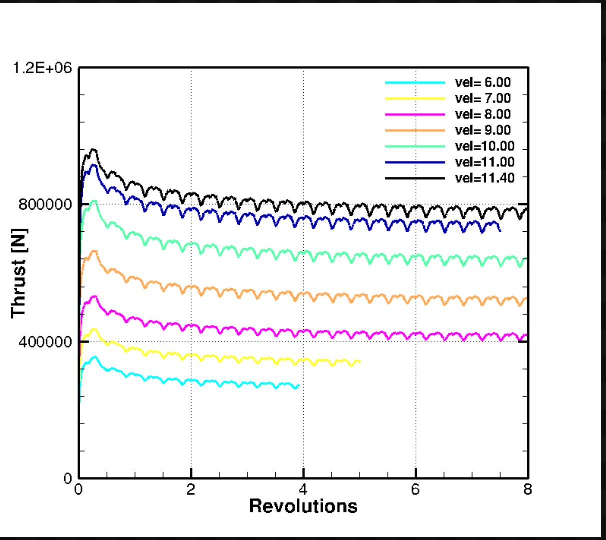

¼° Time Step

Medium Mesh

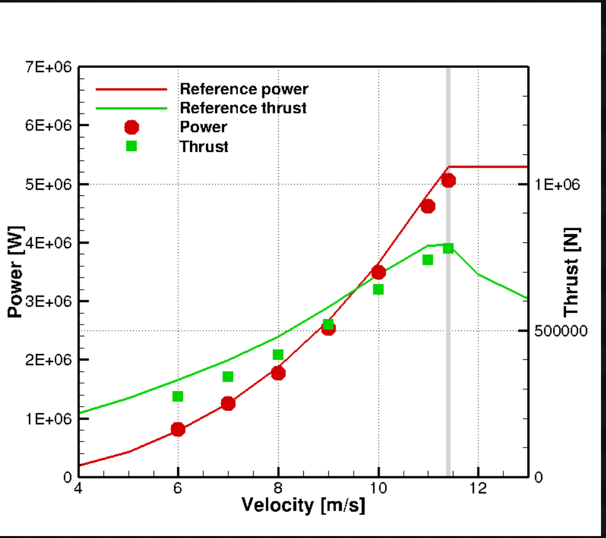

AIAA Paper 2017-3958

Results

- Mesh Resolution Study
  - NREL-5MW
- Single Long Run-Time Study
  - NREL WindPACT-1.5MW
- Single Baseline Turbine Validation
  - Siemens SWT-2.3-93
- Wind Farm Simulation
  - Lillgrund 48 Wind Turbine Farm

NREL WindPACT-1.5MW

2D Cross-Wake Stations

- 7 stations
  - 0.5 – 6.0 rotor diameters (D)
- 160 m x 160 m
  - 400 x 400 (Δx^2: 40 cm x 40 cm)

2,880 Temporal Samples

- 16 rotor revolutions of data
- 2° rotation data frequency
- 31st revolution start

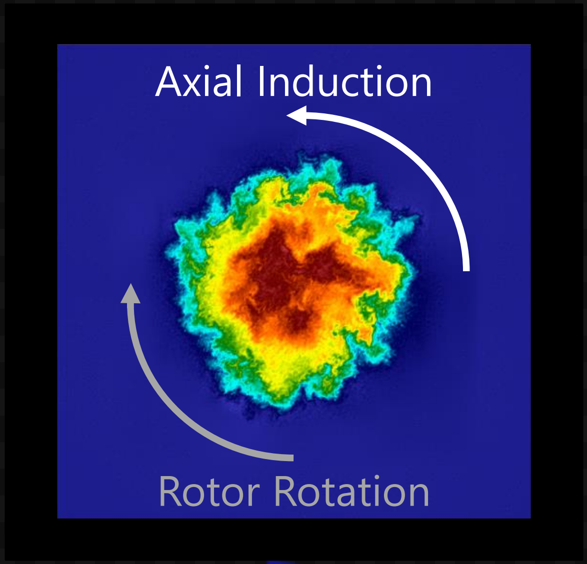

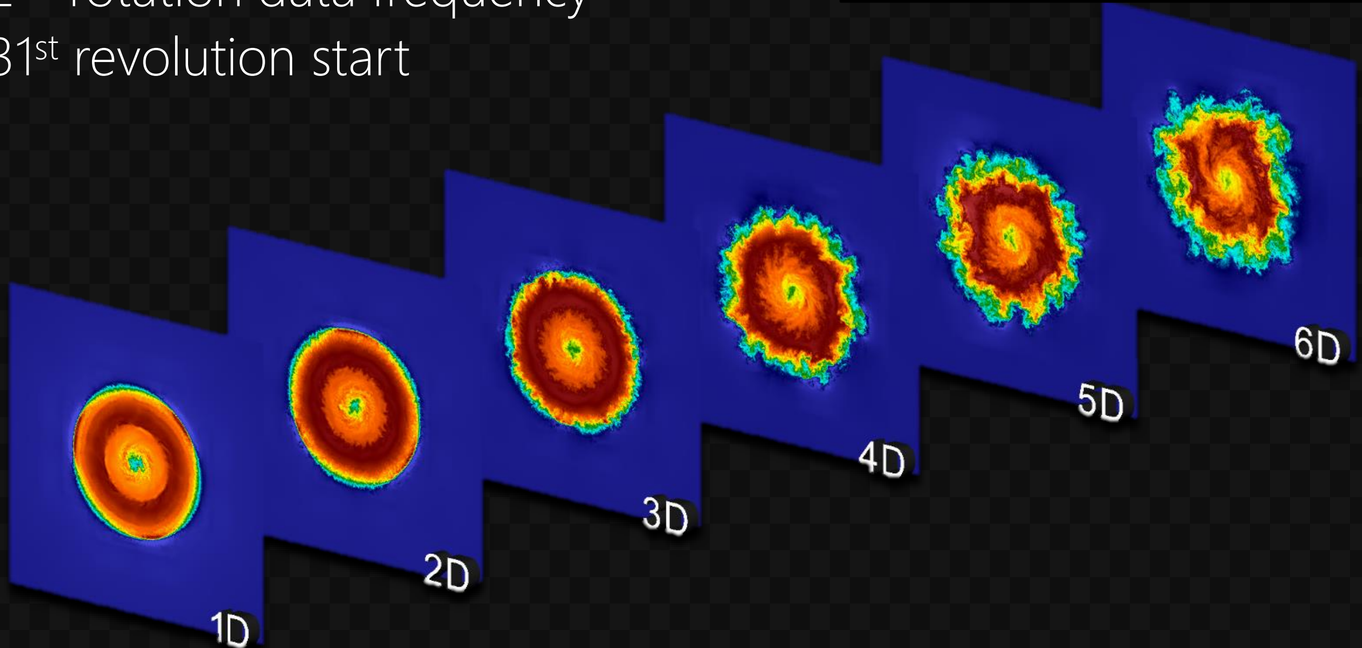

AIAA Paper 2018-0256

Wake Characteristics

Vortex Generation, Merging & Hopping, Breakdown

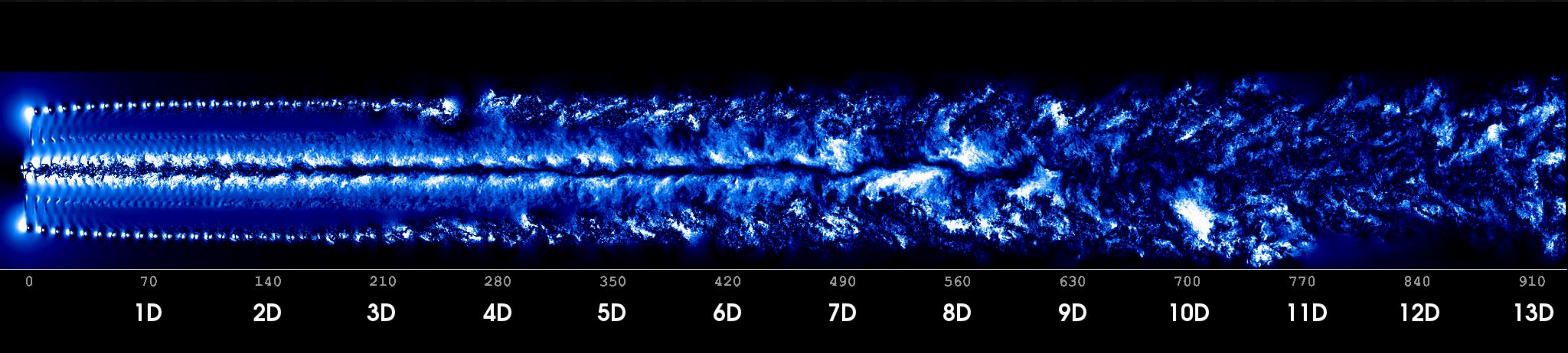

Absolute tangential velocity

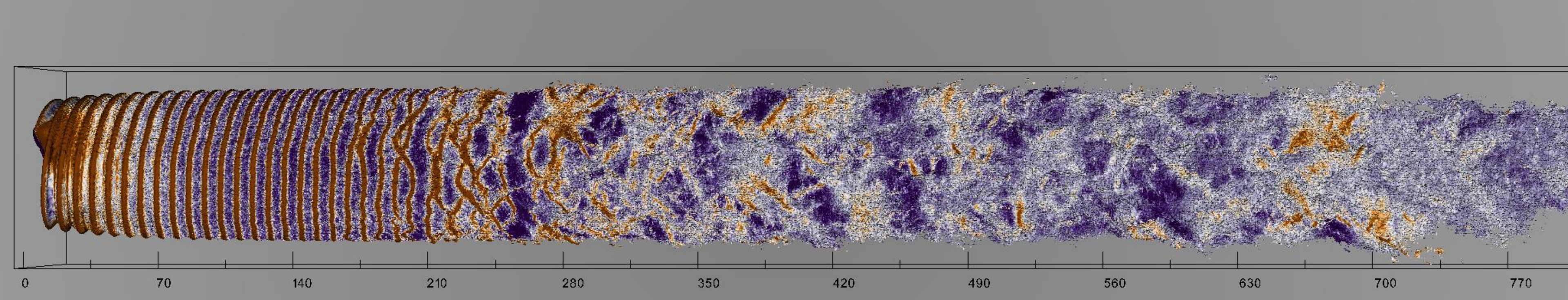

Isocontour of velocity magnitude of 8.5 m/s

AIAA Paper 2018-0256

Wake Breakdown

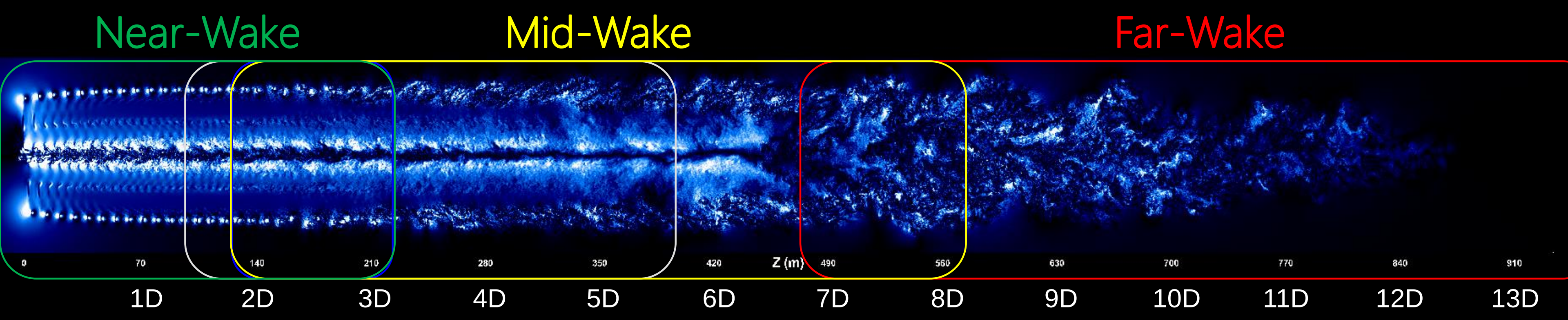

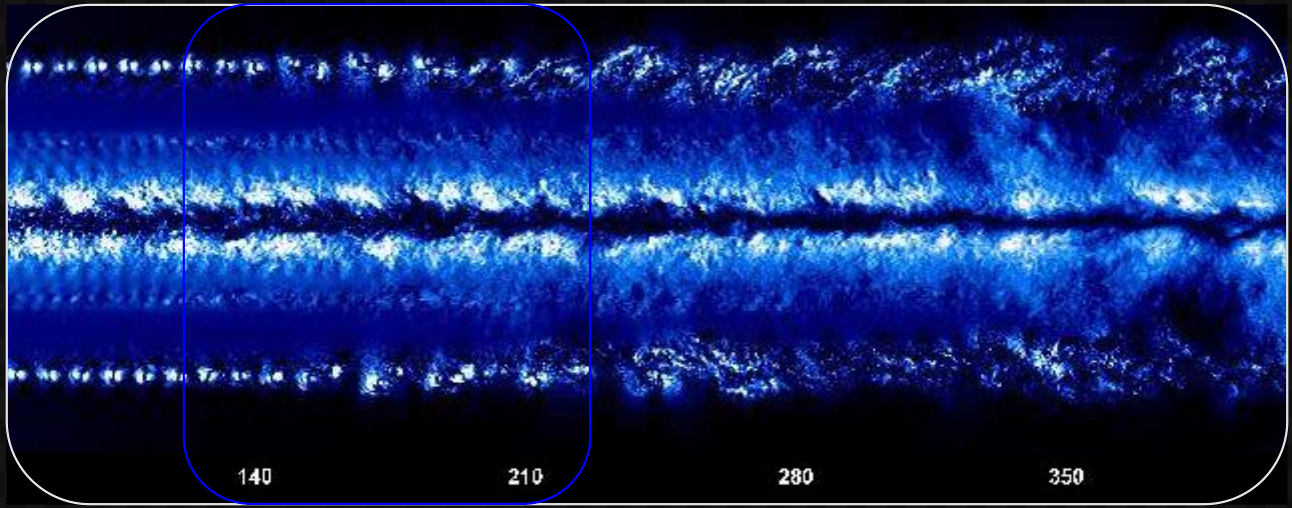

Breakdown Region

Quantify This Region?

AIAA Paper 2018-0256

Proper Orthogonal Decomposition

Axial

Radial

Azimuthal

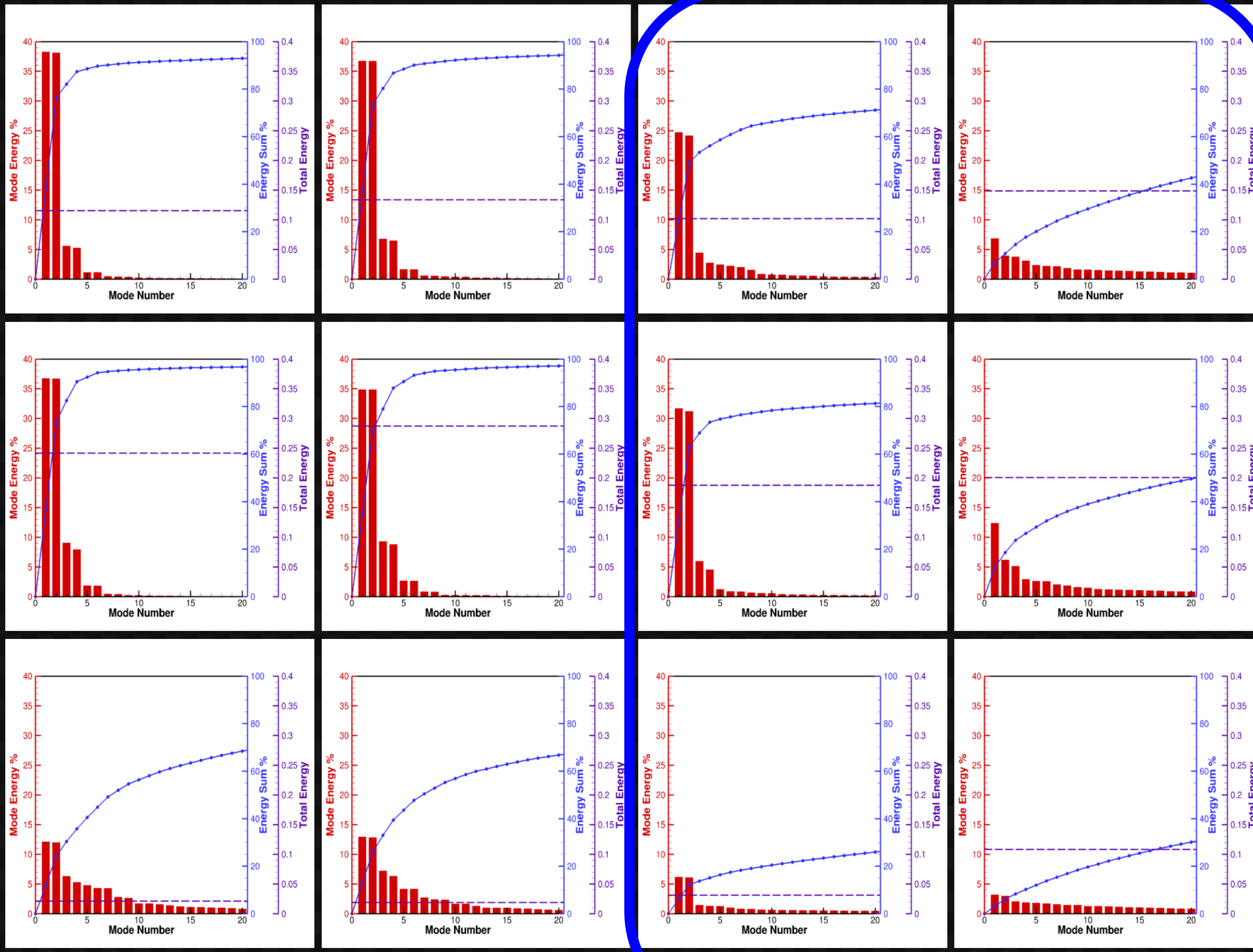

0.5D

1.0D

2.0D

3.0D

Results

Mesh Resolution Study
NREL-5MW

Single Long Run-Time Study
NREL WindPACT-1.5MW

Single Baseline Turbine Validation
Siemens SWT-2.3-93

Wind Farm Simulation
Lillgrund 48 Wind Turbine Farm

Siemens SWT-2.3-93

2.2M grid points per blade
0.5M grid points per tower

- Based on mesh res. study
- Total for Turbine:
  7.1M grid points

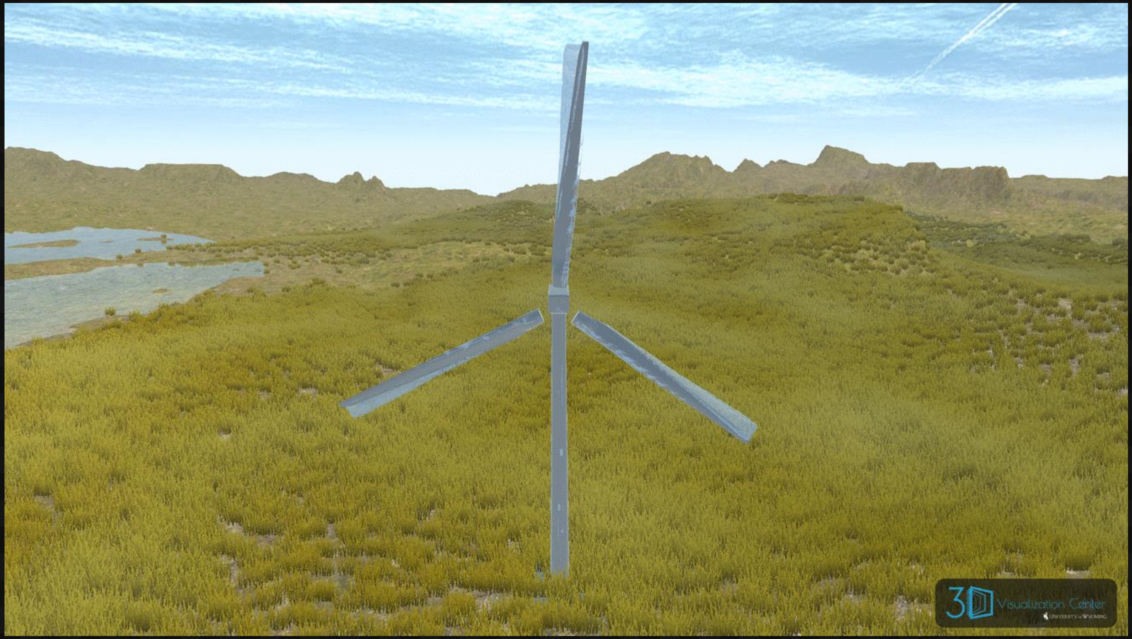

Used for Wind Farm Simulations

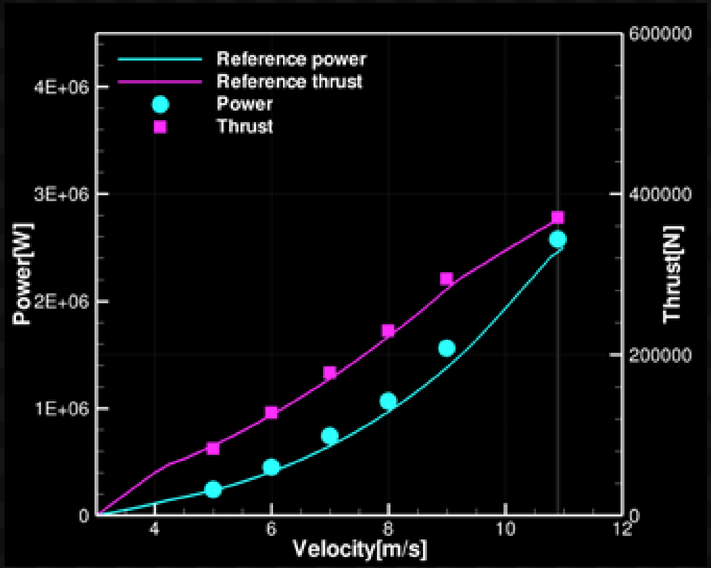

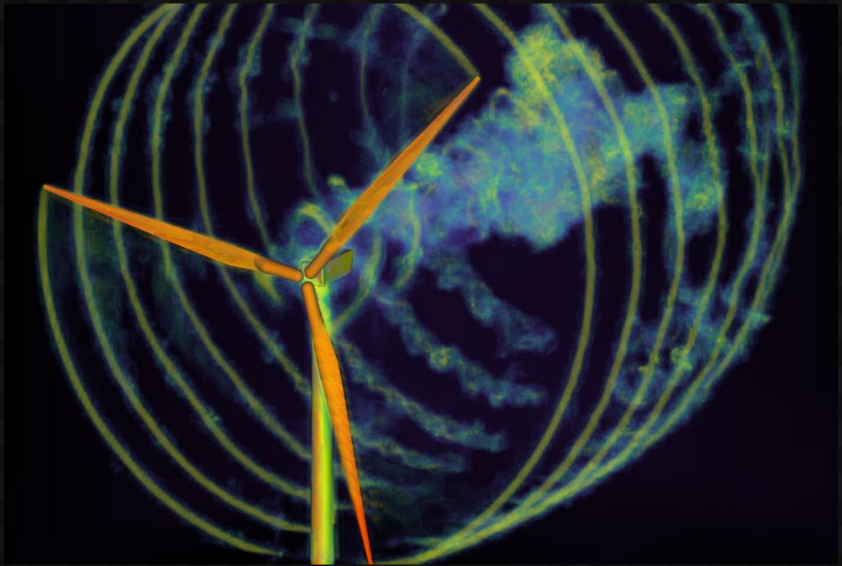

AIAA Paper 2017-3958

Results

- Mesh Resolution Study
  - NREL-5MW
- Single Long Run-Time Study
  - NREL WindPACT-1.5MW
- Single Baseline Turbine Validation
  - Siemens SWT-2.3-93
- Wind Farm Simulation
  - Lillgrund 48 Wind Turbine Farm

Lillgrund Wind Farm

<u>48 Wind Turbines</u>

- 1.55 billion DOFs
- 22,464 cores
- Domain
  10 km x 10 km
- Smallest element in boundary layer
  7E-6 m
- 10 magnitudes of
  spatial scales
- 192 near-body grids
- 360 cores
  (Visualization)

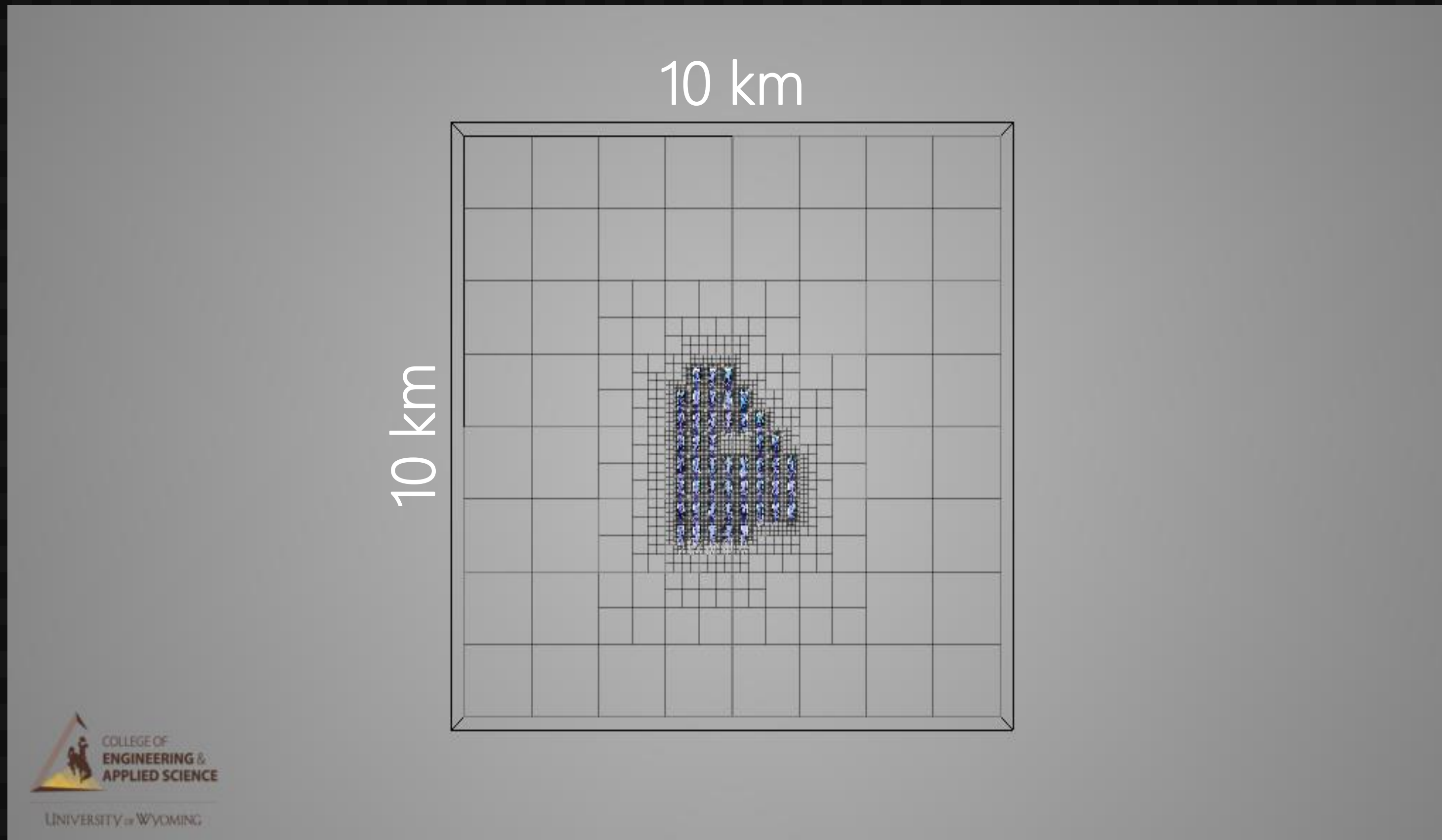

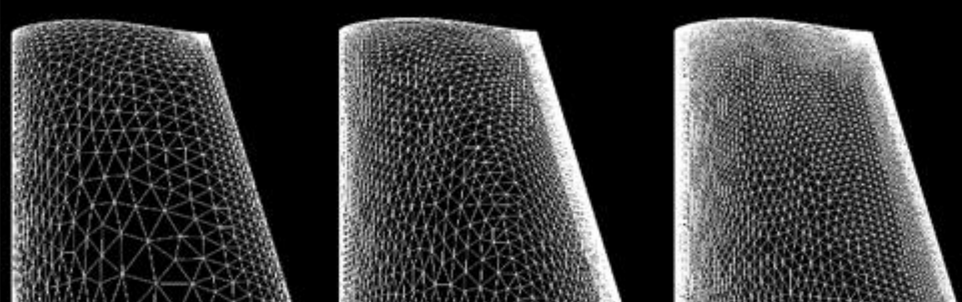

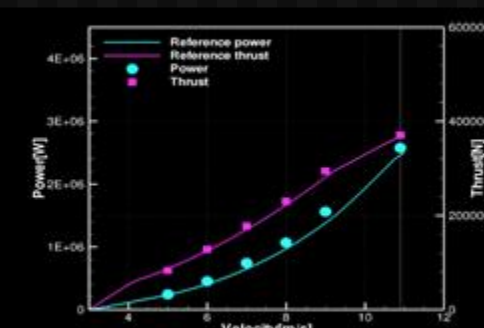

AIAA Paper
2017-3958

Lillgrund Wind Farm

<u>48 Wind Turbines</u>

- 1.55 billion DOFs
- 22,464 cores
- Domain
  10 km x 10 km
- Smallest element in boundary layer
  7E-6 m
- 10 magnitudes of
  spatial scales
- 192 near-body grids
- 360 cores
  (Visualization)

AIAA Paper
2017-3958

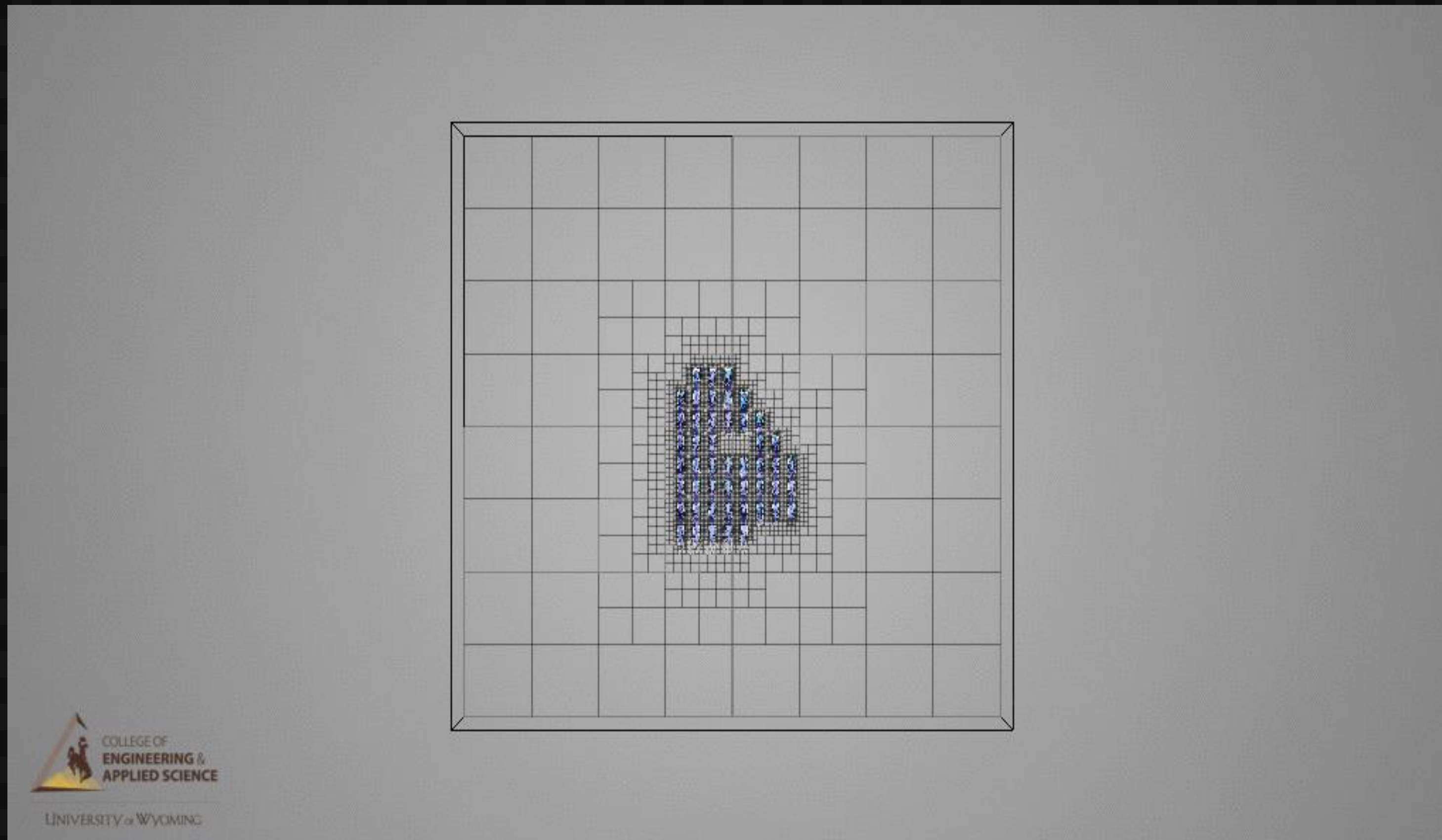

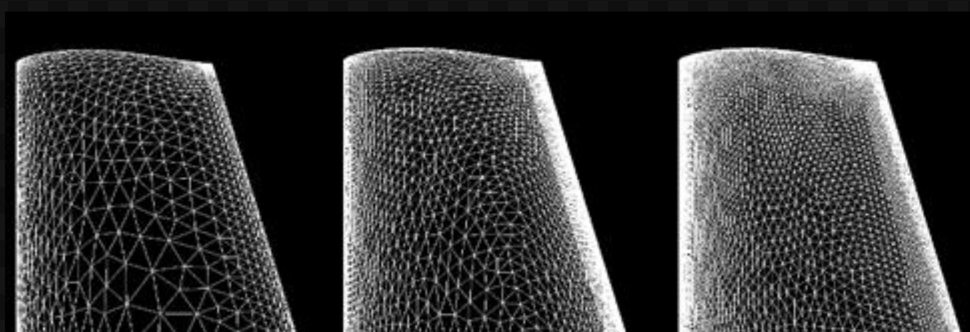

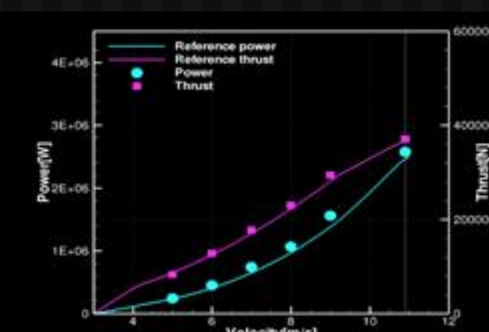

Motivation

Governing Equations

Discretization

Goals

Results

Conclusions

Future Work

Conclusions

Developed DG Method viable for Extreme Scale

- Computational Efficient
- Parallel Scalable
- Robust
- Multiscale
- Real Applications

Largest Overset Simulation

Largest Blade-Resolved Wind Farm Simulation

Enabler of Future CFD Technologies and Reseach

Future Work

Fine-Grain Parallelism

Split Form Method Development

Turbulence Model Development

Error-Based AMR Criterion

Temporal Discretizations

AMR Time Step Sub-Cycling

Atmospheric Boundary Layer Physics

Acknowledgements

Committee

- Dr. Dimitri Mavriplis (Advisor)
- Dr. Victor Ginting
- Dr. Jonathan Naughton
- Dr. Jay Sitaraman
- Dr. Marc Spiegelman

HELIOS Team

- Dr. Andrew Wissink

Mechanical Engineering

- Dr. Michael Stoellinger
- Staff
- Peers

High-Altitude CFD Laboratory

- Dr. Michael Brazell
- Dr. Zhi Yang
- Dr. Behzad Ahrabi
- Dr. Asitav Mishra
- Peers

Friends and Family

- Dr. Rabia Tugce Yazicigil

Mavriplis CFD Lab

Acknowledgements

2016-2017 Blue Waters Fellowship

- NSF Awards OCI-0725070 and ACI-1238993

Compute Time

- NCAR ASD Project
- NCAR-Wyoming Alliance
- UWYO ARCC
- NSF Blue Waters

Office of Naval Research

- ONR Grant N00014-14-1-0045
- ONR Grant N00014-16-1-2737

U.S. Department of Energy, Office of Science, Basic Energy Sciences

- Award #DE-SC0012671

Thank You

Questions?

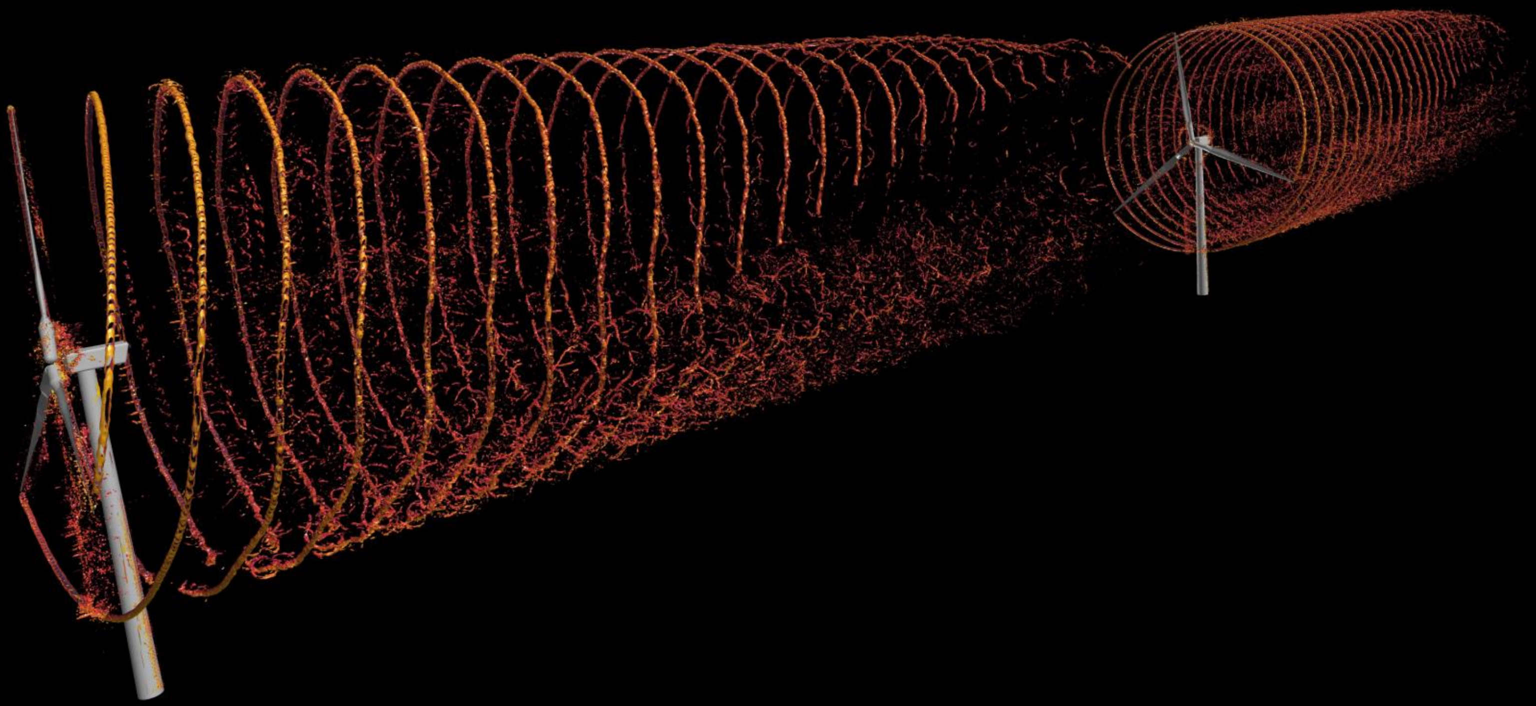

Motivation
Governing Equations
Discretization
Goals
Results
Conclusions
Future Work

Backup Slides

Explicit Runge-Kutta Methods

$$\frac{dy}{dt} = f(t, y) \qquad y_{n+1} = y_n + h\sum_{j=1}^{s} b_j k_j$$

$$\begin{aligned}
k_1 &= f(t_n, y_n), \\
k_2 &= f(t_n + c_2 h, y_n + h(a_{21}k_1)), \\
k_3 &= f(t_n + c_3 h, y_n + h(a_{31}k_1 + a_{32}k_2)), \\
&\vdots \\
k_s &= f(t_n + c_s h, y_n + h(a_{s1}k_1 + a_{s2}k_2 + \cdots + a_{s,s-1}k_{s-1}))
\end{aligned}$$

Butcher Tableau

$$\begin{array}{c|ccccc}
0 & & & & & \\
c_2 & a_{21} & & & & \\
c_3 & a_{31} & a_{32} & & & \\
\vdots & \vdots & & \ddots & & \\
c_s & a_{s1} & a_{s2} & \cdots & a_{s,s-1} & \\
\hline
 & b_1 & b_2 & \cdots & b_{s-1} & b_s
\end{array}$$

$$\begin{array}{c|cc}
0 & & \\
1 & 1 & \\
\hline
 & 1/2 & 1/2
\end{array}$$

(a) SSP-TVD RK2

$$\begin{array}{c|ccc}
0 & & & \\
1 & 1 & & \\
1/2 & 1/4 & 1/4 & \\
\hline
 & 1/6 & 1/6 & 2/3
\end{array}$$

(b) SSP-TVD RK3

$$\begin{array}{c|cccc}
0 & & & & \\
1/3 & 1/3 & & & \\
2/3 & -1/3 & 1 & & \\
1 & 1 & -1 & 1 & \\
\hline
 & 1/8 & 3/8 & 3/8 & 1/8
\end{array}$$

(c) RK 3/8-rule

Split Form Action

$$\sum_{m=1}^{N} 2\mathbf{D}_{im} F^{\#}(\mathbf{Q}_{ijk}, \mathbf{Q}_{mjk})$$

$$F^{\#,1}(\mathbf{Q}_{ijk}, \mathbf{Q}_{mjk}) = \{\{\rho\}\}\{\{u\}\} := \frac{1}{2}\left(\rho_{ijk} + \rho_{mjk}\right) \cdot \frac{1}{2}\left(u_{ijk} + u_{mjk}\right)$$

$$[\mathbf{D}] = [\mathbf{M}]^{-1}[\mathbf{B}] - [\mathbf{M}]^{-1}[\mathbf{Q}]^T$$

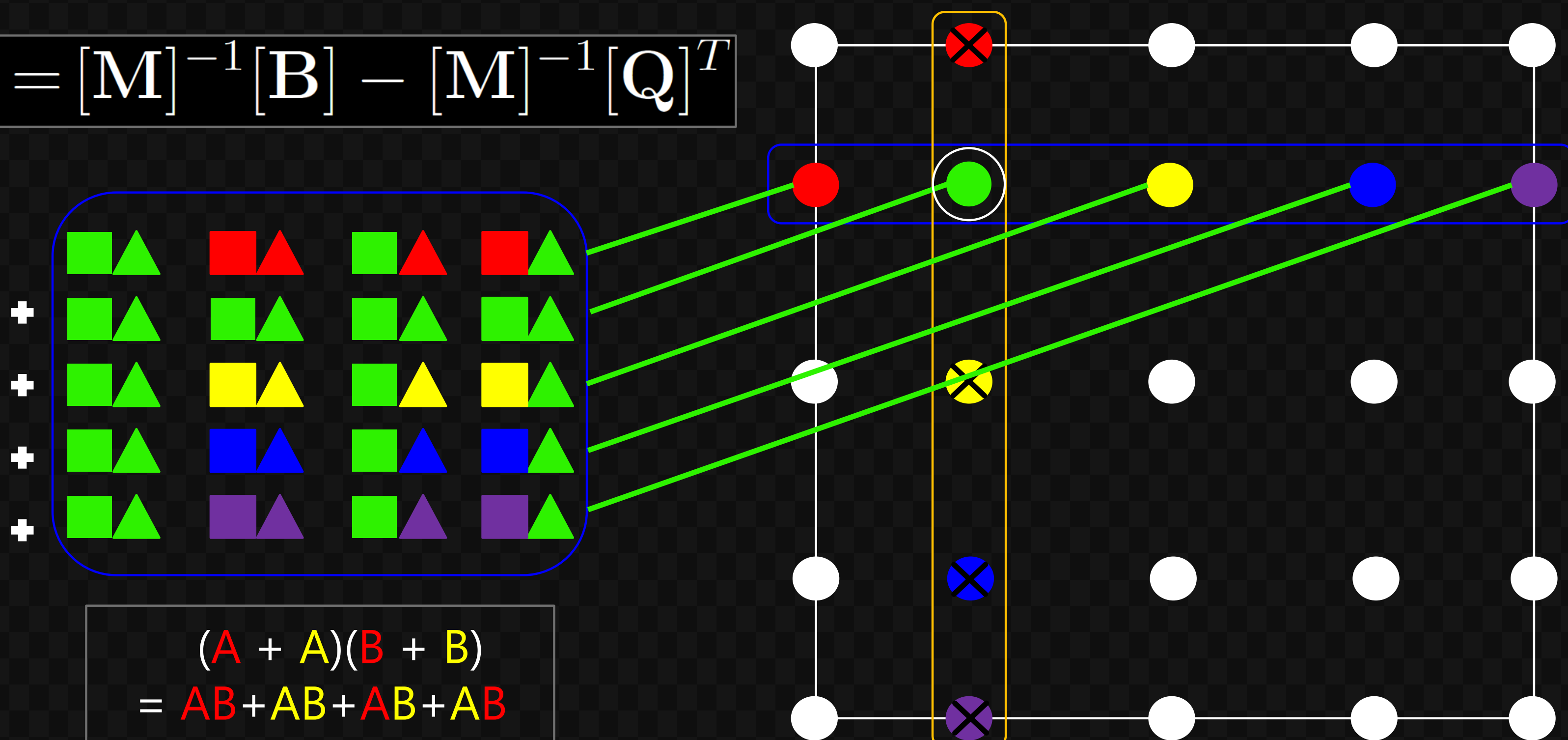

(A + A)(B + B)
= AB+AB+AB+AB

(A + A)(B + B)(C + C)
= ABC+ABC+ABC+ABC+ABC+ABC+ABC+ABC

Patch-Based AMR

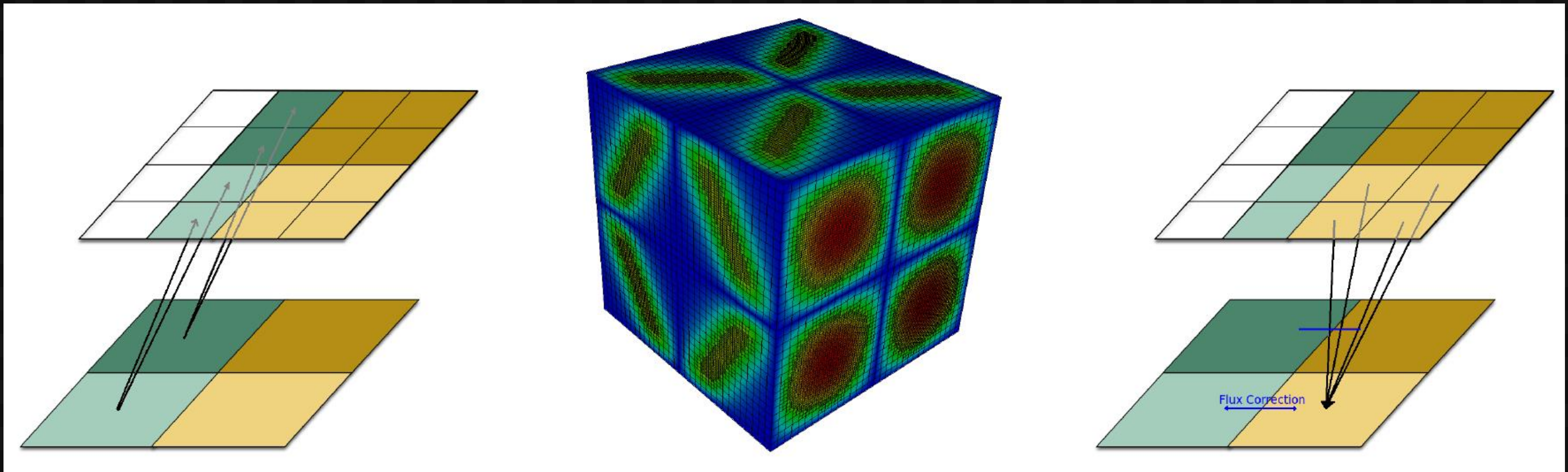

Overset

TIOGA-Topology Independent Overset Grid Assembler

- High-Order interpolation
- Parallel enclosing cell search (donor-receptor) bases on ADT
  - Modified for high-order curved cells
- Interpolation types supported
  - HO FEM to HO FEM
  - HO FVM to HO FEM
  - 2^{nd}-Order FVM to HO FEM
  - 2^{nd}-Order FVM to 2^{nd}-Order FVM

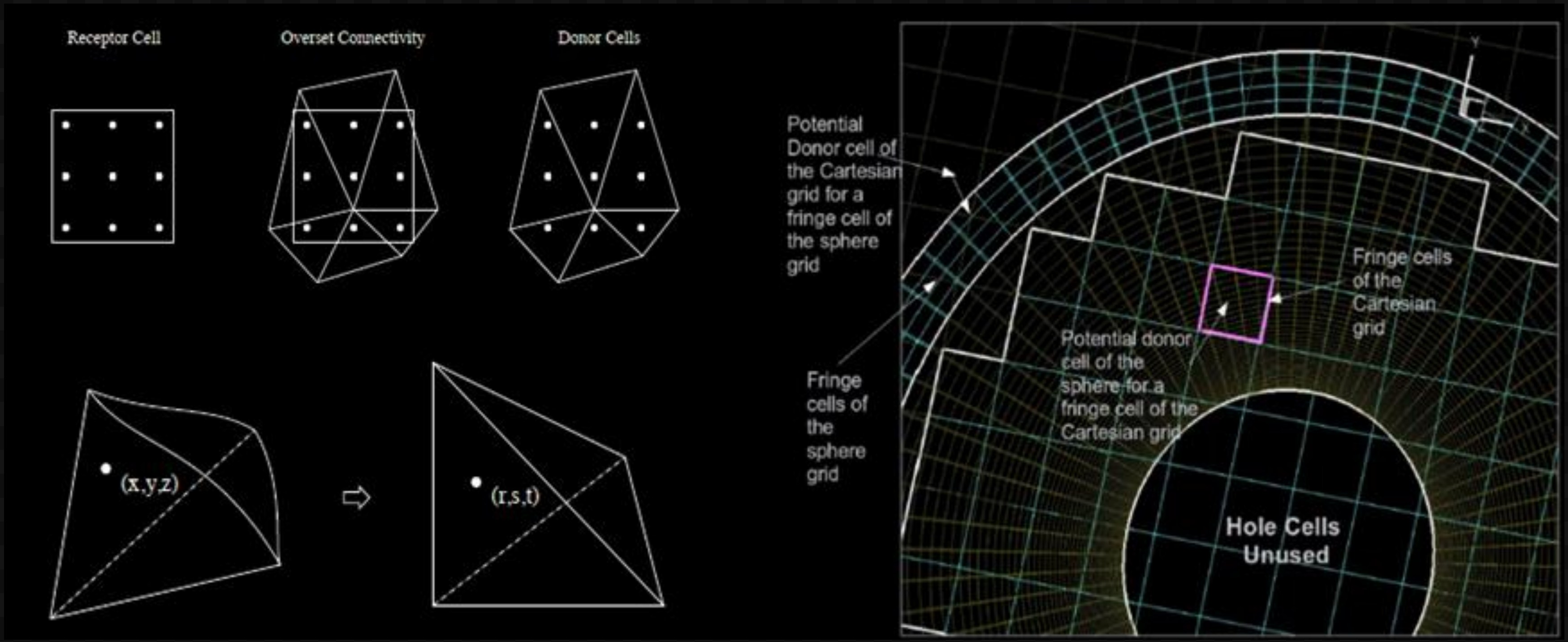

NREL 5MW

Time Refinement Study

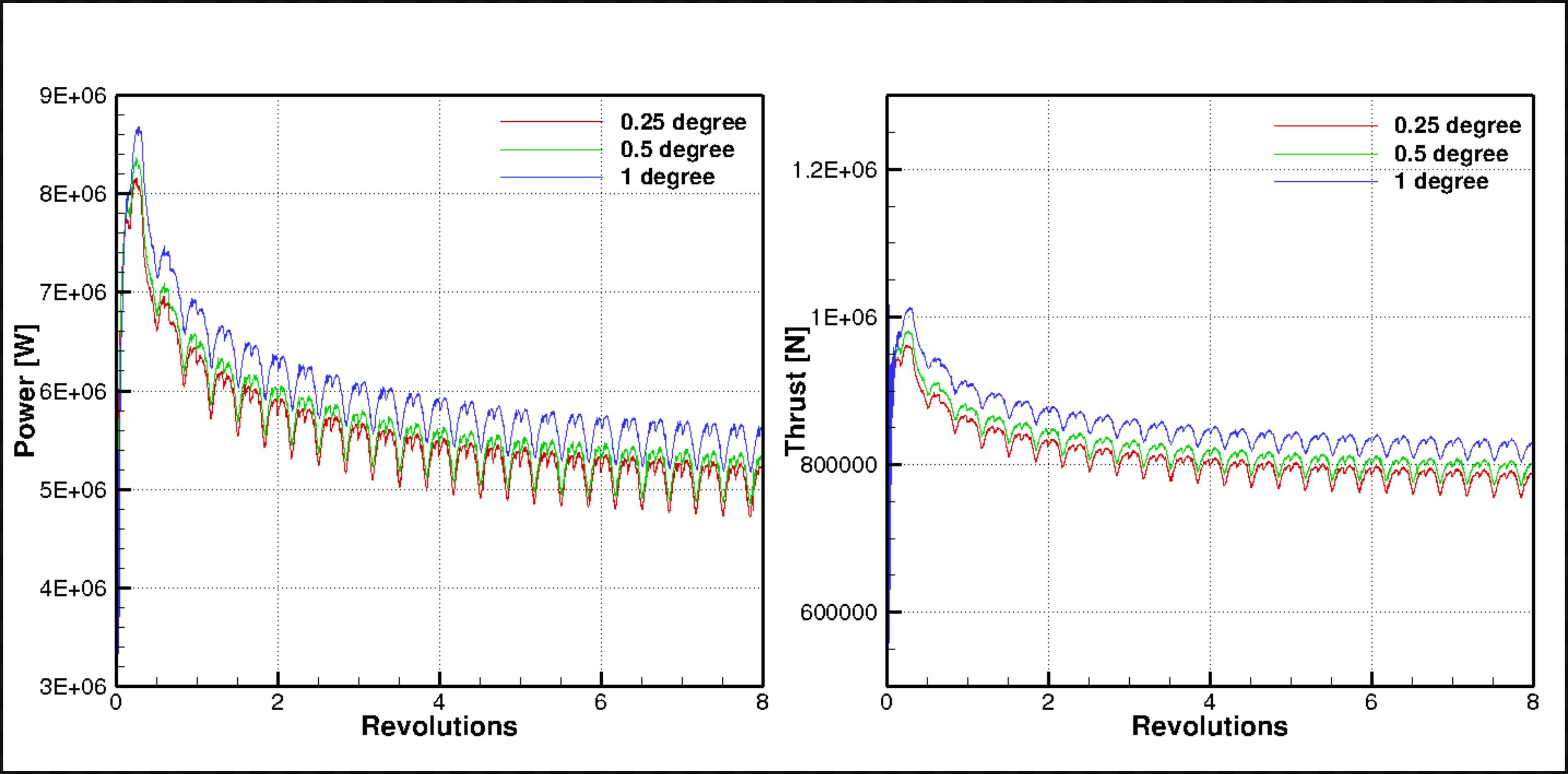

Medium Mesh

AIAA Paper 2017-3958

WAKE3D Scalability

Turbine Count	Efficiency	Revs	Near-Body Cores	Off-Body Cores	Total Cores
6	1.0000	1.374	2,088	720	2,808
12	0.9874	1.360	4,176	1,440	5,616
24	0.9682	1.331	8,352	2,880	11,232
48	0.9333	1.283	16,704	5,760	22,464
96	0.8686	1.194	33,408	11,520	44,928

Near-Body   Off-Body   Overset

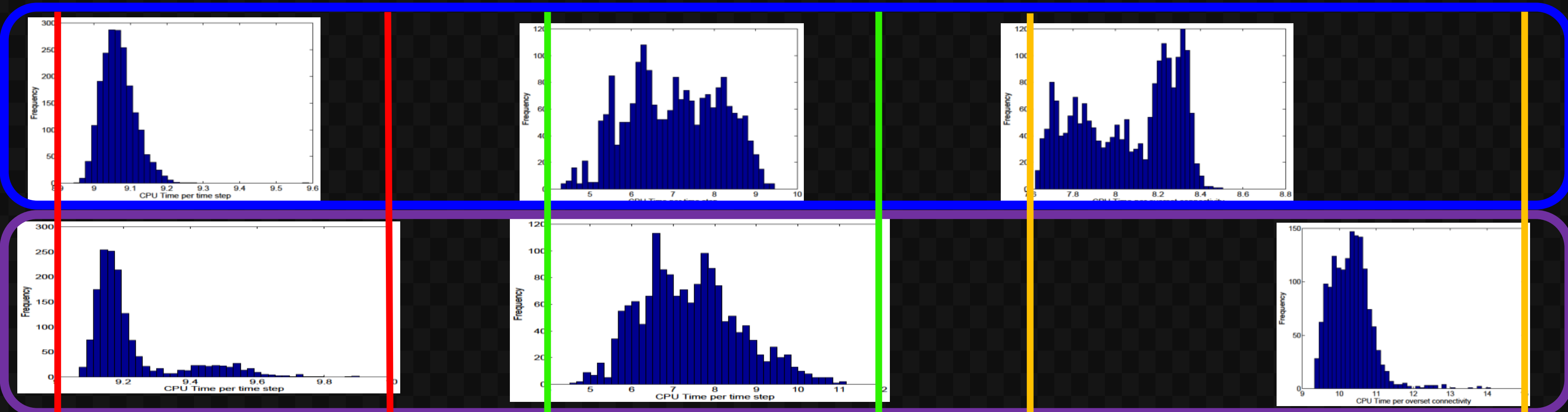

Near-body CPU time   Off-body CPU time   Overset CPU time

6 Turbines   96 Turbines

Atmospheric Inflow Conditions

NCAR WRF

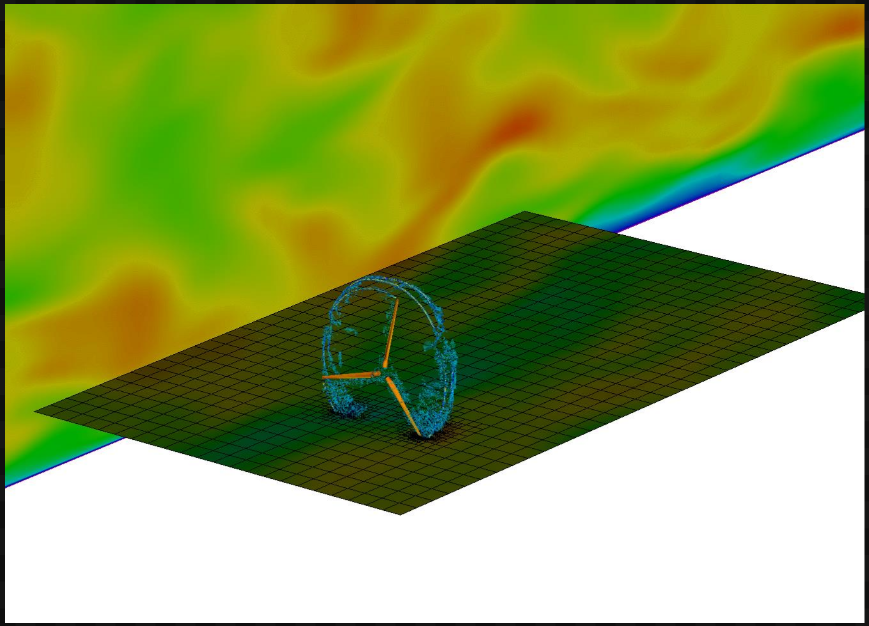

NREL SOWFA

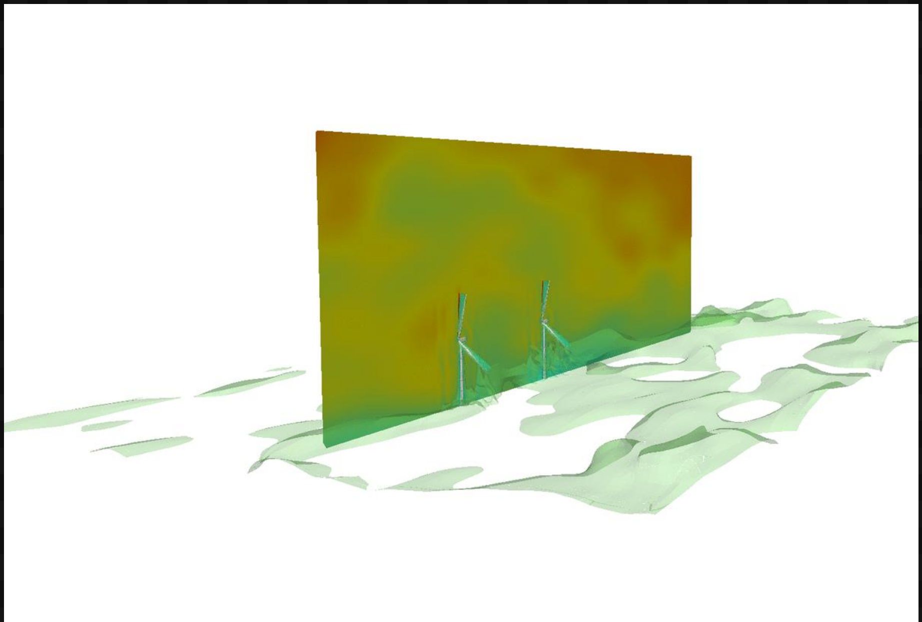

Time Step Sub-Cycling